R-SYMMETRY VIOLATION IN AN ERA OF PRECISION COSMOLOGY

by

Eric Sabo

A thesis submitted to the Faculty of the University of Delaware in partial fulfillment of the requirements for the degree of Master of Science in Physics

Summer 2014

R-SYMMETRY VIOLATION IN AN ERA OF PRECISION COSMOLOGY

by

Eric Sabo

Approved: ____________________________________
Qaisar Shafi, Ph.D.
Professor in charge of thesis on behalf of the Advisory Committee

Approved: ____________________________________
Edmund Nowak, Ph.D.
Chair of the Department of Physics & Astronomy

Approved: ____________________________________
George H. Watson, Ph.D.
Dean of the College of Arts & Sciences

Approved: ____________________________________
James G. Richards, Ph.D.
Vice Provost for Graduate and Professional Education

TABLE OF CONTENTS

Appendix

LIST OF TABLES

LIST OF FIGURES

ABSTRACT

We consider well-motivated particle physics corrections to the standard supersymmetric hybrid inflation scenario. By allowing certain higher order, Planck scale suppressed, R-symmetry violating operators in the superpotential, we are able to give masses to right-handed neutrinos without negatively affecting the down-type quarks. We provide an example with minimal Kähler potential, with the R-symmetry breaking term relevant during inflation being αS^4, where S denotes the well-known gauge singlet inflaton superfield. The inflationary potential takes into account the radiative and supergravity corrections, as well as the soft supersymmetry breaking terms. For successful inflation, with the scalar spectral index in the currently preferred range, $n_s \approx 0.9603$ we find $|\alpha| \lesssim 10^{-7}$. The tensor to scalar ratio $r \lesssim 10^{-4}$, while $|\mathrm{d}n_s/\mathrm{d}\ln k| \sim \mathcal{O}(10^{-3}) - \mathcal{O}(10^{-4})$.

Chapter 1

INTRODUCTION

Humans have been captivated by the cosmos for centuries. Once thought to be a static utopia, we have since come to understand that the universe is anything but. The discovery of the expansion of the universe by Edwin Hubble in 1929 marked the birth of modern cosmology. Perhaps the most famous and most successful development of this field is the Big Bang, or more precisely the *hot* Big Bang - the idea that the universe was born from an incredibly hot and dense space-time singularity.

The Standard Big Bang (SBB) scenario arises naturally by combining Einstein's General Relativity with the assumption that the universe is homogeneous and isotropic. The SBB is extremely successful, but, despite its numerous achievements, the theory suffers from a handful of serious flaws (see section 1.3.3). These plagued the physics community, drawing much criticism, until 1980 when a solution was proposed by Alan Guth [1]. The idea was elegant: a brief period of accelerated expansion in the very early universe, called primordial inflation, or simply *inflation*, could simultaneously solve nearly all of the SBB's problems.

The appeal of such a powerful idea proved enticing to the physics community and the popularity of inflation exploded (see figure 1.1). As with all such theories, however, a number of plausible inflationary models were developed. Practically indistinguishable even ten years ago, today we live in an era of precision cosmology and ever-improving cosmological data allows us to evaluate the past several decades of inflationary research for the first time. While many models have been proven to be unphysical, it is the general opinion of the majority of cosmologists that the inflationary paradigm is here to stay. This view is supported by cosmic microwave background experiments such as the Cosmic Background Explorer (COBE), the Wilkinson Microwave Anisotropy Probe (WMAP) [2], and most recently the Planck satellite [3].

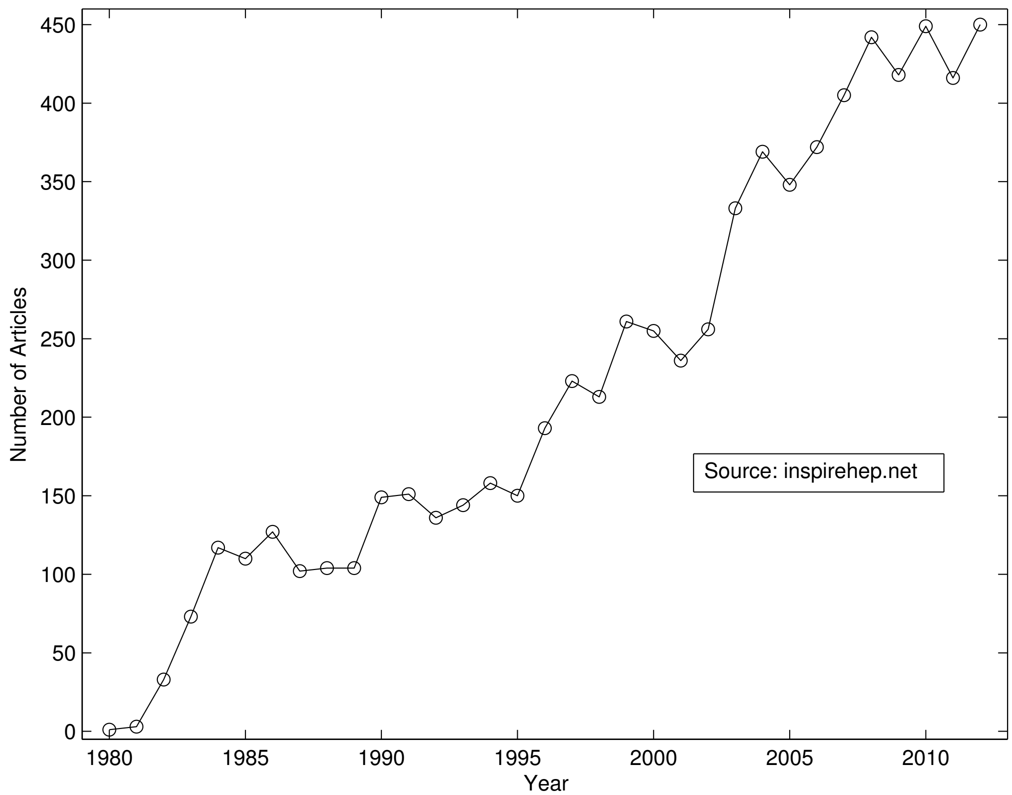

Figure 1.1: Number of articles containing the word "inflation" and its variations in its title published each year since Guth's original paper in 1980. In 2012, there were 450 such articles. Source: `inspirehep.net`. Figure modified from [4].

The goal of inflationary research today is to use cosmological data to guide the development of realistic models. In this thesis, we present one such model. We proceed as follows: The rest of this chapter is devoted to reviewing necessary background material, chapter 2 introduces the concept of inflation through power-law and hybrid inflationary models, and finally, chapter 3 is devoted to original work representing improvements and extensions to the existing theory of supersymmetric (SUSY) hybrid inflation.

1.1 Units And Conventions

Standard high-energy physics units ($\hbar = c = 1$) and notational conventions are employed throughout this work unless otherwise specified. Recall that Greek indices refer to space-time and run over $0, 1, 2, 3$, while Latin indices refer to space alone and run over $1, 2, 3$. Here, the Einstein summation convention is assumed for both Greek and Latin indices, with metric signature $(+, -, -, -)$.

1.2 General Relativity

The underlying framework of modern cosmology is General Relativity (GR). The fundamental object in this theory is the metric tensor $g^{\alpha\beta}$. This is used to define the line element

$$\mathrm{d}s^2 = g_{\alpha\beta}\, \mathrm{d}x^\alpha\, \mathrm{d}x^\beta, \tag{1.1}$$

which represents the distance between two infinitesimally close points on the manifold - a mathematical extension of the concept of a surface to higher dimensions. (Note that $g_{\alpha\beta}$ is the inverse of $g^{\alpha\beta}$.) Derived from the metric are the Christoffel symbols,

$$\Gamma^\alpha_{\gamma\beta} = \frac{1}{2} g^{\alpha\delta} \left(\frac{\partial g_{\gamma\delta}}{\partial x^\beta} + \frac{\partial g_{\delta\beta}}{\partial x^\gamma} - \frac{\partial g_{\gamma\beta}}{\partial x^\delta} \right), \tag{1.2}$$

which are coordinate-dependent expressions for the Levi-Civita connection. These take into account the effects of parallel transport on the manifold. Derived from the connection is the Ricci (curvature) tensor,

$$R^\alpha_\beta = g^{\alpha\gamma} \left(\frac{\partial \Gamma^\delta_{\gamma\beta}}{\partial x^\delta} - \frac{\partial \Gamma^\delta_{\gamma\delta}}{\partial x^\beta} + \Gamma^\delta_{\gamma\beta}\Gamma^\sigma_{\delta\sigma} - \Gamma^\sigma_{\gamma\delta}\Gamma^\delta_{\beta\sigma} \right), \tag{1.3}$$

which describes the deviation of the manifold from Euclidean space. Finally, derived from the Ricci tensor is the Ricci scalar, $R = R^\alpha_\alpha$. Also known as the scalar curvature, it is the simplest curvature invariant of a Riemannian manifold.

These combine to form the geometric components (left hand side) of the Einstein-Hilbert field equations,

$$G^{\alpha}_{\beta} \equiv R^{\alpha}_{\beta} - \frac{1}{2}\delta^{\alpha}_{\beta} R = \frac{T^{\alpha}_{\beta}}{{m_P}^2}, \tag{1.4}$$

which say that the presence of mass-energy curves space-time, and particles follow geodesics in curved space-time. Here, $m_P = 1/\sqrt{8\pi G} \approx 2.43 \times 10^{18}$ GeV is the reduced Planck mass and G is Newton's gravitational constant. Here, the discrete Kronecker-Delta is defined in the usual sense, $\delta^{\alpha}_{\beta} = \mathrm{diag}(1,1,1,1)$. The matter components (right hand side) of (1.4) are determined by the energy-momentum tensor T^{α}_{β}. Appropriate choices of $g^{\alpha\beta}$ and T^{α}_{β} may be used to study the space-time evolution of the universe and are our starting points for studying the SBB.

1.3 Standard Big Bang

The SBB is a collection of topics describing how the universe came to be in its present state. At the heart of this is the elegant merger of two very different fields: particle physics and cosmology. On one hand, there is the expanding universe governed by GR, while on the other hand, there are diverse topics such as Big Bang nuclearsynthesis, baryogensis, leptogenesis, preheating and reheating, and the cosmic microwave background all mainly governed by particle physics. Here we provide a brief review of a collection of SBB topics that play a role and serve to motivate the next two chapters on inflation.

1.3.1 The Expanding Universe

The governing equations for an expanding universe follow from the Einstein equations (1.4). The assumption of the *cosmological principle* - the *observable* universe is homogenous and isotropic on large scales - provides a unique choice for $g^{\alpha\beta}$ called the Robertson-Walker metric. In spherical coordinates, $x^{\alpha} = (t, r, \theta, \phi)$, this produces the line element

$$\mathrm{d}s^2 = \mathrm{d}t^2 - a^2(t)\left[\frac{\mathrm{d}r^2}{1-kr^2} + r^2\left(\mathrm{d}\theta^2 + \sin^2\theta\,\mathrm{d}\phi^2\right)\right], \tag{1.5}$$

where k is either $-1, 0$, or 1 depending on the curvature of space-time, and $a(t)$ is called the (dimensionless) scale factor. The known constituents of the universe have no viscosity or heat flow, which allows them to be characterized as perfect fluids. This leads to the relativity simple form of the energy-momentum tensor with respect to the rest frame of the fluid: $T^{\alpha}_{\beta} = \mathrm{diag}(\rho, -p, -p, -p)$, where ρ represents the total energy density of the universe and p a pressure. Putting this all together produces the *Friedmann equation*,

$$\left(\frac{\dot{a}}{a}\right)^2 = \frac{1}{3{m_P}^2}\rho - \frac{k}{a^2}, \tag{1.6}$$

the *acceleration equation*,

$$\frac{\ddot{a}}{a} = -\frac{1}{6{m_P}^2}(\rho + 3p), \tag{1.7}$$

and the *fluid equation*

$$\dot{\rho} + 3\frac{\dot{a}}{a}(\rho + p) = 0, \tag{1.8}$$

where dots represent derivatives with respect to ordinary time t. The first two of these are the 00-component and the trace of (1.4), respectively, while the third equation may be derived by combining the Friedmann and acceleration equations. It is often convenient to introduce the Hubble parameter $H \equiv \dot{a}/a$, which will come in handy beginning in chapter 2.

The pressure is provided through an equation of state $p \equiv p(\rho)$, which uniquely depends on each possible constituent in the following way:

- **Dust:** Also known by "(non-relativistic) matter," dust refers to any constituent which exerts negligible pressure, and it is a good approximation for cool atoms. In this case, $p = 0$.

- **Radiation:** Highly-relativistic particles, such as photons and neutrinos, may be shown to exert a radiation pressure equal to $p = \rho/3$.

(Note that had we not taken $\Lambda = 0$ in equation (1.4), we would also have another equation of state corresponding to a "cosmological constant".) It is easy to show that the cosmic dynamics of universes with more than one constituent are governed by whichever constituent is most dominant at the time. For example, if radiation were most important, we find

$$a(t) \propto t^{1/2} \quad , \quad \rho_{\rm rad} \propto t^{-2} \quad , \quad \rho_{\rm dust} \propto a^{-3} \propto t^{-3/2}.$$

On the other hand, if dust were more important, we find

$$a(t) \propto t^{2/3} \quad , \quad \rho_{\rm rad} \propto a^{-4} \propto t^{-8/3} \quad , \quad \rho_{\rm dust} \propto t^{-2}.$$

From these results, we may conclude that the universe is expanding.

1.3.2 Cosmic Microwave Background

One of the most successful features of the Standard Big Bang is the prediction of the cosmic microwave background (CMB), predicted in 1948 by Ralph Alpher and Robert Herman and discovered by Penzias and Wilson in 1964 [5]. The origin of the CMB occurs when the universe was approximately 1/1000-th of its present size and was an incredibly hot, dense sea of electrons and ions. At this time, atoms were not able to form because the energy of a typical photon was much greater than the ionization energy of hydrogen. However, as the photons redshifted to lower energies due to the expansion of the universe, they could no longer continue to prevent electrons from bonding. This process is called *decoupling* and occurred when the universe was $\sim$ 3000 K. Having lost their ability to interact with ordinary matter, these decoupled photons have been traveling the universe ever since and are currently in the form of microwaves at 2.7 K. First measured by COBE in 1992 [6–8], measurements of the CMB continue today via experiments such as WMAP and Planck. The most famous of these measurements is the CMB temperature anisotropy (see figure 1.2), which justifies the assumption of homogeneity and isotropy in the Robertson-Walker metric of section 1.3.1.

The key feature of the CMB is that it allows us to look at the universe at a young age. Consequently, measurements of the CMB may be used as a method of experimental verification of cosmological models of the early universe. Two important

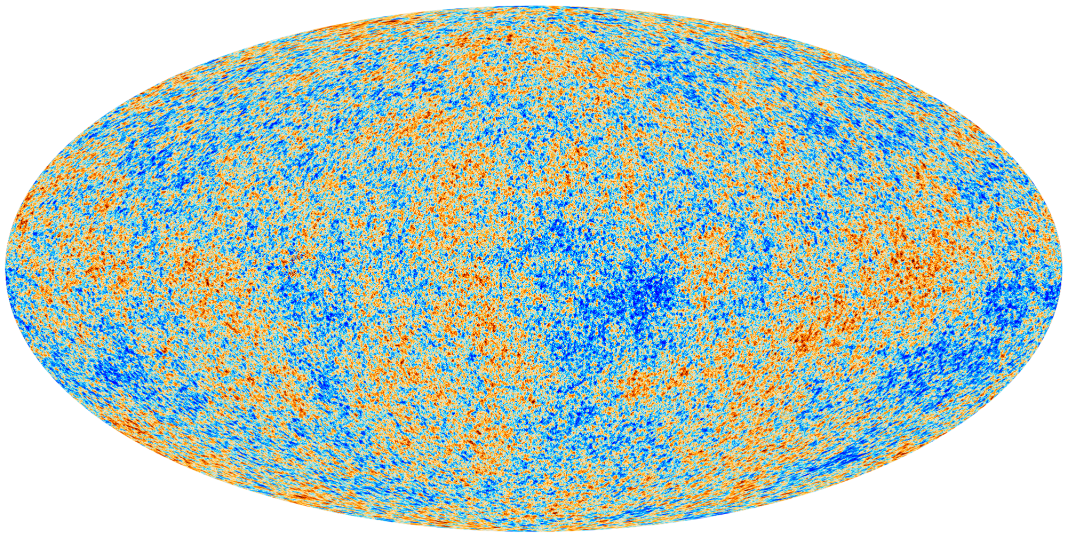

Figure 1.2: The CMB anisotropies at decoupling as observed by Planck [3].

measurements related to this work are the determination of the power spectrum and polarization. We will put these in context in chapter 2, but for the moment it suffices to say that the three observables derived from these two measurements are able to rule out and distinguish between inflationary models.

1.3.3 Problems Of The SBB

Despite the incredible success of the SBB, there are three problems that the theory cannot explain. Here we provide a brief explanation of each. The solution to these problems is called inflation and is the topic of the following chapters.

The Flatness Problem

An important feature of the Friedmann equation (1.6) is its dependence on the space-time curvature k. The values -1, 0, or 1 for k represent perfectly open, flat, or closed universes, respectively. Solving the Friedmann equation with $k = 0$ shows that a perfectly flat universe stays perfectly flat throughout the evolution of the universe. However, solving the Friedmann equation with a small perturbation from zero shows that even the slightest deviation from flat gets amplified into increasingly non-zero curvature as the universe expands. Mathematically, $k = -1$ and $k = 1$ are said to be stable, while $k = 0$ is said to be unstable. This instability creates a problem as current measurements dictate that the universe is (incredibly close to) perfectly flat [9]. The SBB scenario has no explanation for why out of all the possible values for k, the universe seems to have chosen k exactly 0. This is called *the flatness problem*.

It is convenient while discussing the flatness problem mathematically to cast the Friedmann equation (1.6) into the form

$$|\Omega - 1| = \frac{k}{a^2 H^2}, \tag{1.9}$$

where

$$\Omega(t) = \frac{\rho}{\rho_c}$$

is the density parameter defined with respect to the critical density

$$\rho_c(t) = 3H^2 {m_P}^2$$

If $k = 0$, then $\Omega = 1$ is constant for all time; hence $\Omega = 1$ represents an extremely fine-tuned solution. Current evidence suggests that Ω is extremely close to one.

The Horizon Problem

One of the most profound philosophical implications of the SBB is that the universe has a finite age. Combining this with the fact that the speed of light is finite implies that photons could have only traveled a finite distance since the Big Bang. Referring to figure 1.2, this implies that points on the left hand side would not have had enough time to reach points on the right hand side. Each point in figure 1.2 is contained in a domain, or horizon, which represents the maximum distance light from that point could have traveled since the Big Bang. Thermal equilibrium requires that each domain "communicate" with each other, but this could not have happened. So then how is it possible that the entire CMB is at approximately the same temperature? This is called *the horizon problem*. It may be shown that the horizon problem is directly related to the flatness problem.

The Monopole Problem

A key concept in high energy physics is that of symmetry breaking (see section 1.4). Physically, symmetry breaking is associated with phase transitions, such as those that occur naturally in the SBB as the universe cools due to expansion. However, as before in the horizon problem, we can't expect the entire universe to cool the same way, as not all domains are causally connected. The natural question to ask in this case is: What happens when two previously uncorrelated domains come into connect? In this case, there is a domain A with one set of properties, a domain B with potentially a different set of properties, and a boundary that separates them. Depending on how different the two sets of properties are, rather abrupt things can happen on the boundary. This is called a topological defect. Such features are not present in the Standard Model (SM), but are common in most SM extensions, such as those discussed in sections 1.4 and 1.5. To this day, no conclusive evidence as to the existence of topological defects has ever been found [10].

Mathematically, topological defects are solitonic solutions of the classical field equations. More importantly, they interpolate between vacuum states of the field. As such, they are directly related to the topology of the vacuum manifold. To see this, consider a simplified model given by

$$\mathcal{L} = \frac{1}{2}\partial_\mu \phi \, \partial^\mu \phi - \frac{\lambda}{4}\left(\phi^2 - \sigma^2\right)^2,$$

where $\phi = (\phi^1, \phi^2, \ldots, \phi^n)\,, n = 0, 1, 2, \ldots$. The minimum of the potential is described by

$$\phi^2 = \left(\phi^1\right)^2 + \left(\phi^2\right)^2 + \ldots + \left(\phi^n\right)^2 = \sigma^2.$$

When $n = 1$, the minimum is at $\phi = \pm\sigma$, which may be identified with the 0-sphere S^0. Now suppose we have a domain A that goes to $\phi = \sigma$; domain B has no information about A and goes to $\phi = -\sigma$ with probability $1/2$. However, the field is continuous on $[-\sigma, \sigma]$ and therefore must vanish at some point in between. This happens on the surface $\phi(x^i) = 0$, which is called a domain wall. When $n = 2$, the minimum is at $(\phi^1)^2 + (\phi^2)^2 = \sigma^2$, which may be identified with a circle, or 1-sphere S^1. As before, suppose ϕ^1_A, $\phi^2_A > 0$ and ϕ^1_B, $\phi^2_B < 0$ with probability 1/4. Continuity implies that ϕ^1 and ϕ^2 vanish on surfaces $\phi^1(x^i) = 0$ and $\phi^2(x^j) = 0$, respectively. The intersection of these two-dimensional surfaces defines the curve $\phi^1 = \phi^2 = 0$, and is called a cosmic string. This leads to a false vacuum in the potential. When $n = 3$, the minimum is at $(\phi^1)^2 + (\phi^2)^2 + (\phi^3)^2 = \sigma^2$, which may be identified with the 2-sphere S^2. A false vacuum is created at the intersection of the three surfaces $\phi^i(x^j) = 0$. These are called monopoles. The procedure is a little more involved for $n = 4$, but these are called textures. These concepts are demonstrated in figure 1.3.

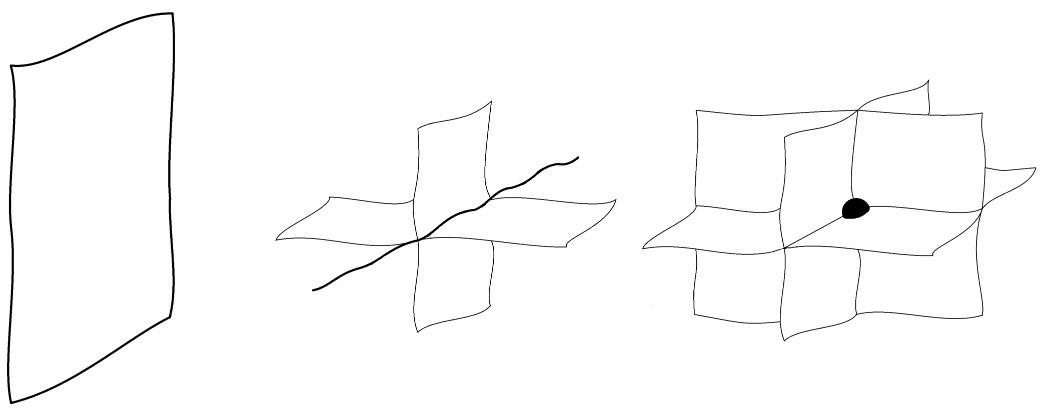

(a) (b) (c)

Figure 1.3: (a) Domain wall; (b) Cosmic string; (c) Monopole. Figure adapted from [11]

Let us make the above discussion more rigorous. Consider the three paths found in figure 1.4. We say path A is homotopic to path B because path A can be continuously deformed into path B through a collection of intermediate paths, each of which lies in Ω, while keeping its endpoints fixed. Conversely, path A is not homotopic to path C because such a continuous deformation is not possible due to the presence of the hole. This classification partitions Ω into equivalence classes, from which we obtain the first homotopy group, also called the fundamental group, $\pi_1(\Omega)$. Intuitively, π_1 contains information about the "defects" of Ω, such as the presence of the hole seen in figure 1.4. This idea may be generalized to the n-th homotopy group, $\pi_n(\mathcal{M})$, formally defined as the set of homotopy classes of maps from the n-sphere S^n to $\mathcal{M}$, where $\mathcal{M}$ is a topological space.[1]

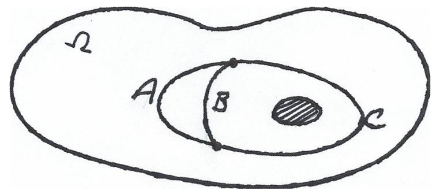

Figure 1.4: Path A is homotopic to path B because path A can be continuously deformed into path B through a collection of intermediate paths, each of which lies in Ω, while keeping its endpoints fixed. Conversely, path A is not homotopic to path C because such a continuous deformation is not possible due to the presence of the hole.

Armed with this new machinery, one may show that topological defects are formed when the n-th homotopy group of the vacuum manifold $\mathcal{M}$ is nontrivial, i.e., $\pi_n(\mathcal{M}) \neq \mathbf{0}$. The vacuum manifold $\mathcal{M}$ is defined as the quotient group H/G, which denotes the breaking of the group H to the subgroup G. (More on this in section 1.4.) In practice, determining the homotopy groups π_n is not easy. Fortunately, the following result holds for all the scenarios we need consider here: If $\pi_n(H)$ and $\pi_{n-1}(H)$ are both trivial, then $\pi_n(H/G) = \pi_{n-1}(G)$. Using this and the fact that $\pi_n(S^n) = \mathbb{Z} \neq \mathbf{0}$, we may apply the techniques of homotopy theory to the examples of topological defects above. The results are collected in table C.1. (See appendix C for a collection of useful results used in making table 1.1.)

Each of the four types of topological defects found above: domain walls, cosmic strings, monopoles, and textures carry certain physical properties. For example, the properties of defects such as cosmic strings were once considered vital to the formation of large scale structures in the early universe, but this idea is no longer supported by

[1] In general, one may consider maps to topological spaces other than S^n, however, these have little relevance to our discussion.

n	$\mathcal{M}$	Homotopy Group	Topological Defect
1	S^0	$\pi_0(S^0)$	Domain wall
2	S^1	$\pi_1(S^1)$	Cosmic string
3	S^2	$\pi_2(S^2)$	Monopole
4	S^3	$\pi_3(S^3)$	Texture

Table 1.1: Topological defects as related to homotopy groups of the vacuum manifold.

the data [10]. Electroweak symmetry breaking is related to a doublet of complex scalar fields ($n = 4$), however, the textures involved here prove uninteresting. On the other hand, the monopoles generated by phase transitions in an expanding universe are of great interest in high-energy physics. It may be shown that these topological defects carry a magnetic charge that correspond to Dirac monopoles at field positions far from the center of the monopole.

While this property of magnetic monopoles is of extreme importance in theoretical physics, their existence creates a problem for the SBB. According to this, magnetic monopoles should be immensely abundant in the universe today. But if this were true, why haven't we detected them? The situation gets even worse when we consider realistic particle physics scenarios, such as those in sections 1.4 and 1.5, where symmetry breaking is common and leads to the formation of defects via the Kibble mechanism [12] - the mechanism responsible for defect production in the early universe due to phase transitions in the Higgs field. In addition to the four topological defects defined above, realistic theories may produce hybrid defects such as strings with monopoles on the ends (called necklaces). Clever mechanisms may be devised to reduce the number of defects produced, but the fact is that, for the most part, magnetic monopoles are unavoidable in theories containing $U(1)_{\mathrm{EM}}$. This is called *the monopole problem.*

1.4 Grand Unified Theories

While the success of the Standard Model (SM) is unparalleled by any other theory of physics, it is clear today that it is not the last word. For starters, it does not include gravity, a viable dark matter candidate, or neutrino masses, and is rather complicated and somewhat arbitrary. Physicists have worked over the past several decades to "replace" the SM with a more complete and theoretically pleasing theory. Here we are interested in an idea that originated in the 1970's called *grand unification*.

To demonstrate the idea of grand unification, consider the SM local-symmetry group G, most often called the gauge group. This is a compact Lie group on a finite-dimensional Hilbert space V. (This is in contrast to the global-symmetry group of quantum field theory called the Poincaré group, which is a noncompact Lie group on an infinite-dimensional Hilbert space.) Since V is finite-dimensional, we may decompose it into a direct sum of irreducible representations, or simply irreps for short. Mathematically we may identify the fundamental fermions as basis vectors of irreps and gauge bosons as group actions.

In this respect, the term unification represents the following. Let G be a subgroup of some larger group H. The irreps of H on V may be larger than the irreps of G when H is restricted to G. These larger irreps of H restricted to G allow particles to be unified further than they would be in the smaller irreps of simply G. The term grand unification is used when G is simple, i.e. not a product of other groups.

Examples of grand unified theories (GUTs) include Howard Georgi and Sheldon Glashow's $SU(5)$ [13] and Georgi's $Spin(10)$ [14]. (This is sometimes called by the name $SO(10)$, but the true symmetry group here is $Spin(10)$, the double cover of $SO(10)$.) Both theories extend the SM symmetry group $SU(3)_c \times SU(2)_L \times U(1)_Y$. The $SU(5)$ theory extends to $Spin(10)$ either directly or through the $SU(4) \times SU(2) \times SU(2)$ Pati-Salam model [15]. We'd want to do this for several reasons, but most importantly because minimal $SU(5)$ has been ruled out, while $Spin(10)$ is still a viable GUT candidate.

In general, predictions of GUTs improve with the addition of supersymmetry (SUSY) (section 1.5). GUTs without SUSY fail to solve the doublet-triplet problem or dynamically break the electroweak symmetry via radiative corrections. GUTs may also have model specific problems, such as rapid proton decay in $SU(5)$, which may be improved by incorporating SUSY. Unfortunately, in this specific case, minimal SUSY $SU(5)$ still has a proton decay problem with dimension five operators.

Here we are interested in $Spin(10)$ and a modification of the $SU(5)$ theory called flipped $SU(5)$ or anti $SU(5)$ [16]. As previously mentioned, $Spin(10)$ is still a viable GUT candidate, but implementing successful cosmological models in this theory is not straightforward. One problem is that $Spin(10)$ leads to the formation of stable topological defects via the Kibble mechanism (see section 1.3.3) in a manner that is not solvable by inflation.

On the other hand, SUSY hybrid inflation (see chapter 3) scenarios result naturally as a consequence of breaking the extra $U(1)_{B-L}$ symmetry embedded in $Spin(10)$, and have been shown to produce results consistent with current particle phenomenology. This works as follows, instead of breaking to the SM symmetry group directly, $Spin(10)$ is first broken to an intermediate group, such as flipped $SU(5)$. At this point false vacuum hybrid inflation occurs, followed by the breaking of the intermediate group to the SM. This approach has the benefit of implementing hybrid inflation without extra external fields, symmetries, or fine tuning. The choice of the intermediate group and the manner in which $Spin(10)$ breaks to it may be used to avoid some of the problems of topological defect creation mentioned above (see for example [17]).

The flipped $SU(5)$ theory is given by $SU(5) \times U(1)_X$. By adding the extra copy of $U(1)$, we are able to write the particle charge operator Q as a linear combination of generators in $SU(5)$ and $U(1)_X$. This has the effect of creating relationships between matter and antimatter that provide different proton decay predictions than in standard $SU(5)$. Including supersymmetry suppresses the troublesome dimension five operators via a $U(1)$ R-symmetry.

From an inflationary perspective, we are interested in flipped $SU(5)$ for two main reasons. First, flipped $SU(5)$ naturally lacks monopole defects [18], which makes it natural to consider the breaking $Spin(10) \rightarrow$ flipped $SU(5) \rightarrow$ SM. Second, the same $U(1)_R$ provides a unique renormalizable superpotential using only the minimal Higgs sector, which has been shown to produce successful inflationary scenarios. As a result, we mainly adopt flipped $SU(5)$ as our gauge group throughout this work, with little regard as to whether or not it is playing the part of an intermediate group.

Fortunately, in inflation we don't directly care about the particle irreps themselves; we need only concern ourselves with the dimensionality of the representation of the field. This is denoted by $\mathcal{N}$, and often appears while considering radiative corrections to the scalar potential. This number is model specific and may be different under $Spin(10)$ and flipped $SU(5)$ depending on the scenario.

1.5 Supersymmetry

At the time of writing, there is no definite evidence of physics beyond the SM; however, it is highly suggested (see section 1.4). Another SM extension we are interested in here is SUSY, which also, as with GUTs, originated in the early 1970's. Today, SUSY is considered the leading contender to solve the hierarchy problem [19] - the apparent difference between gravity and the other forces - and is able to accurately predict the mass of the recently discovered Higgs boson [20]. As the name suggests, in addition to the symmetries present in the SM, SUSY extends Lorentz invariance, which creates a new symmetry that creates a relationship between fermions and bosons. Mathematically, this forces supersymmetric operators to obey a specific algebra. The resulting irreps create supermultiplets containing both fermonic and bosonic states called superpartners. Working out the properties of the supermultiplets, we find the familiar particles but also new supersymmetric particles as well. These have not yet been discovered.

Supersymmetry comes in two forms: global and local. Global supersymmetry is what is usually referred to by "SUSY", while local supersymmetry is called *supergravity*, or SUGRA for short. For the purposes of this work, the most important difference between the two is that SUSY is renormalizable, while SUGRA is not. Since the universe is inherently non-renormalizable, SUGRA is the true form of supersymmetry chosen by nature. However, renormalizable field theories may be thought of as approximations of non-renormalizable theories, and in this regard, global SUSY is usually a good approximation to SUGRA. In general, this holds true whenever taking m_P to infinity is okay. In inflation this limit does not make sense [21], so we have to invoke SUGRA corrections to SUSY to take into account physics near the Planck scale.

The main motivation to include SUSY in a theory of inflation is due to the necessity of having elementary scalar fields - invoking SUSY avoids the quadratic divergences in the masses of the elementary light scalar fields. A number of non-SUSY inflationary theories are still consistent with current data [22], but they are more difficult to motivate from a consistent particle physics standpoint. The most widely considered versions of supersymmetry are the Minimal Supersymmetric Standard Model (MSSM) and Next To Minimal Supersymmetric Standard Model (NMSSM). The first is the minimal extension to the Standard Model that includes supersymmetry, while the latter includes an extra singlet "chiral" superfield (useful in solving the μ-problem [23]). The MSSM and the NMSSM are considered "$N = 1$" (one group generator) supersymmetry because they contain one supersymmetric transformation. The chiral supermultiplets in $N = 1$ theories contain a spin-0 complex scalar fields and a spin-1/2 chiral fermion field, while gauge supermultiplets contain a spin-1 gauge field and a spin-1/2 gaugino field.

There are different ways to mathematically represent SUSY, but it is convenient in the context of this work to use the superfield formulation. This allows us to write down a Lagrangian with respect to the superfields in the same way we would in classical field theory for regular fields. This Lagrangian is given by

$$\mathcal{L} = \int \mathrm{d}^2\theta \, W(Z_i) + \int \mathrm{d}^4\theta \, K(Z_i, Z_i^\dagger), \tag{1.10}$$

where we have neglected terms not relevant to this work. Here, W is called the superpotential of the superfields Z_i, K is called the Kähler potential[2], and θ is a Grassmannian coordinate. Considering the dimensions of each term, it may be shown that the form of W and K is limited. This will be important for us later.

[2] The Kähler potential is related to the curvature of the Kähler manifold which describes field space.

The fact that SUSY is not readily detected means that the underlying symmetry must be broken in nature. Global SUSY may be broken "explicitly" or "softly", whereas SUGRA, being a local symmetry, must be spontaneously broken. The energy scale at which this happens is related to the gravitino mass - the spin-3/2 superpartner of the spin-2 gravitron - by $2\sqrt{6\pi}\, m_P\, m_{3/2}$ [24]. This breaking is assumed to occur in the so-called "hidden sector". For our purposes, the hidden sector is assumed to communicate via gravity only weakly with the "visible sector" - the fields with the SM gauge interactions. Hence, we say that this theory is *gravity-mediated*. All of this refers to the true vacuum. SUSY is required to be broken during inflation, but this breaking may not necessarily be related to breaking in the true vacuum. In this work we use a special type of SUSY-breaking called *soft SUSY-breaking*. This happens in the visible sector at an energy scale $m_{3/2}$. As it turns out, only certain soft SUSY-breaking terms are allowed. This will be important in chapter 3.

As we will see in chapter 2, inflation requires a scalar potential, so we must extract this information from equation (1.10). The formula to do this involves so-called "F-terms" and "D-terms":

$$F_i = -\left(\frac{\partial W}{\partial Z_i}\right)^* \quad , \quad D = \frac{g}{2} \sum_i q_i \, |Z_i|^2 \, .$$

Here, g is a coupling and q_i is the field's charge under the appropriate symmetry. From these we get the scalar potential $V = V_{\mathrm{F}} + V_{\mathrm{D}}$,

$$V_{\mathrm{F}} = \sum_i |F_i|^2 \quad , \quad V_{\mathrm{D}} = \frac{1}{2}\, D^2.$$

(Note that here the superfields are replaced by their scalar components z_i.) It is easy to show that supersymmetry is spontaneously broken if and only if an F or D term is nonzero. Recall that this formula does not involve K because the Kähler potential only appears in the kinetic terms. Including just the D-terms produces unsatisfactory inflationary scenarios, while just the F-terms produce models that are easy to motivate and naturally satisfy current experimental constraints. Including both terms can satisfy experiments, but such models are often overly complicated.

There are a lot of possible fields in SUSY, however, we only consider some of them in inflation model building. As a result, the inflationary superpotential is independent of some fields, while others are held fixed at the origin. These are called "flat directions". In this work, we choose what is called "D-flatness" and use an F-term only model. This becomes important when we approach the Planck scale where we must include SUGRA corrections. The F-term SUGRA potential is given by

$$V_F = e^{K/m_P^2}\left[\left(\frac{\partial W}{\partial z_i} + m_P^{-2}\frac{\partial K}{\partial z_i}W\right)K_{ij}^{-1}\left(\frac{\partial W}{\partial z_i} + m_P^{-2}\frac{\partial K}{\partial z_i}W\right)^* - 3m_P^{-2}\left|W\right|^2\right], \quad (1.11)$$

where

$$K_{ij} \equiv \frac{\partial^2 K}{\partial z_i \partial z_j^*}.$$

As corrections, these terms are small and it suffices in our case to expand (1.11) in powers of m_P^{-1} and suppress terms much below double floating point precision.

To go any further, we must specify a form for W and K. Unfortunately, supersymmetry does not provide much insight into this area. The Kähler potential is a real function of the fields and their complex conjugates, however, it is easy to show that W must be analytic (holomorphic). This restricts the forms of allowed terms but not tremendously. One may also impose a number of different symmetries, both discrete and continuous, to forbid unwanted terms such as those involved in proton decay. It is standard to impose that W satisfy certain internal symmetries which may or may not alter its phase. This is valid since the overall phase of W is unphysical. Internal symmetries which alter the phase of the superpotential are called R-symmetries and are of great importance in this work. (More on this in chapter 3.)

For more information on the above topics, the reader is referred to any text or review on supersymmetry. Notable references include [25] and [26].

Chapter 2

INFLATION

Technically, the flatness, horizon, and monopole problems are not fatal to the Standard Big Bang scenario (SBB). If the initial conditions of the early universe are fine-tuned enough, the SBB works perfectly. For example, the universe could have happened to have been created perfectly flat. From a theoretical standpoint, however, this kind of thinking is rather unappealing. Inflation is an elegant solution to these problems which does not require fine-tuning. Roughly speaking, inflation is defined as a period of *accelerated* expansion, ($\ddot{a} > 0$). The universe is currently in a state of accelerated expansion, but by inflation we mean primordial, or cosmological, inflation, which is theorized to occur between $\sim 10^{-36}$ and $\sim 10^{-33} - 10^{-32}$ seconds after the Big Bang and have expanded the universe by $\sim 10^{78}$ in volume.

Taking place so close to the Big Bang naturally puts inflation in the realm of *ultra* high energy physics with an energy scale of $\sim 10^{16} - 10^{18}$ GeV. (For comparison, the Large Hadron Collider has an expected peak energy of a mere $\sim 10^{4}$ GeV.) Thus, any theory of inflation represents a substantial extrapolation of the laws of physics as we understand them today. Fortunately for us, if it occurred, inflation is predicted to have left behind numerous traces of its existence, allowing us to make *testable* predictions of physics well beyond the grasp of future particle accelerators. So far, current generation experiments such as the WMAP and Planck satellites have observed several cosmic relics, all of which support modern inflationary theory.

Inflation model building has a special place in high energy theory because it is a link between particle physics and cosmology. A successful theory of inflation must explain where inflation comes from and how it ends. The particle associated with inflation is called the inflaton and is described by a scalar field as a phase transition.

This particle is required to decay into the Standard Model (SM) particles at the end of inflation during preheating and reheating such that the SBB can begin. These processes are not yet completely understood and are the topic of active research.

The first true model of inflation was proposed in 1980 by Guth [1], but is no longer considered viable. This model has been dubbed *old inflation* to distinguish it from viable models of inflation that were first proposed in 1982 by Linde [27] and Albrecht and Steinhardt [28]. Here we give a brief review of these models.

2.1 Inflation As A Solution

As previously promised, a period of accelerated expansion solves the problems of the SBB (section 1.3.3). Let's start with the flatness problem. The condition for inflation implies

$$\ddot{a} > 0 \quad \Longrightarrow \quad \frac{\mathrm{d}}{\mathrm{d}t}\left(\dot{a}\right) > 0 \quad \Longrightarrow \quad \frac{\mathrm{d}}{\mathrm{d}t}(aH) > 0.$$

Looking back at (1.9), regardless of the initial value of the curvature k, an inflating universe drives the right-hand side to zero:

$$|\Omega - 1| = \frac{k}{a^2 H^2} \quad \Longrightarrow \quad |\Omega - 1| = 0 \quad \Longrightarrow \quad \Omega = 1.$$

Inflation also solves the horizon problem, as the expansion of the universe due to inflation is enough to expand an initially small region in thermal equilibrium to sizes much larger than the observable universe. Thus, the horizon problem is avoided because the region in figure 1.2 was originally in thermal equilibrium to begin with. Likewise, inflationary expansion is enough to dilute the density of any unwanted relics such as topological defects; hence solving the monopole problem.

2.2 Inflationary Dynamics

The part of the action related to inflationary dynamics, called the inflationary sector, is given by

$$S_{\text{inf}} = \int \mathrm{d}^4x\sqrt{-g}\left[\frac{1}{2}g^{\mu\nu}\partial_\mu\phi\,\partial_\nu\phi - V(\phi)\right], \tag{2.1}$$

where $g = \det(g^{\mu\nu})$, and ϕ is the inflaton. This could include coupling to other fields (see section 2.4) and contain non-canonical kinetic terms, but we will not discuss these here. The energy-momentum tensor for ϕ is

$$T_{\mu\nu} = -\frac{2}{\sqrt{-g}}\frac{\delta S_{\text{inf}}}{\delta g^{\mu\nu}} = \partial_\mu\phi\,\partial_\nu\phi - g_{\mu\nu}\left(\frac{1}{2}\partial^\sigma\phi\,\partial_\sigma\phi + V(\phi)\right).$$

For reasons we will not go into, we only care about the homogenous mode of the field, i.e., $\phi(t,x) = \phi(t)$. With this, assuming the Robertson-Walker metric (1.5) forces $T_{\mu\nu}$ into the form of a perfect fluid with

$$\rho = \frac{1}{2}\dot{\phi}^2 + V(\phi)$$
$$p = \frac{1}{2}\dot{\phi}^2 - V(\phi),$$

where dots represent derivatives with respect to ordinary time t. From here we see it is possible for ϕ to have a negative pressure if the potential dominates the kinetic energy, $\frac{1}{2}\dot{\phi}^2 \ll V(\phi)$. In this case, the Friedmann equation (1.6) becomes

$$H^2 \approx \frac{1}{3m_P^2}V(\phi), \tag{2.2}$$

where $H = \dot{a}/a$ is the Hubble parameter. (Note that the condition $\ddot{a} > 0$ corresponds to $H > 0$. Also, obtaining a negative pressure is key to inflationary theory because the condition $\ddot{a} > 0$ implies that $\rho + 3p < 0$ in the acceleration equation (1.7), and density is always taken to be positive.)

Varying (2.1) with respect to ϕ produces

$$\frac{\delta S_{\text{inf}}}{\delta\phi} = \ddot{\phi} + 3H\dot{\phi} - \nabla^2\phi + \frac{\delta V}{\delta\phi} = 0, \tag{2.3}$$

Choosing ϕ homogenous as before, the Laplacian vanishes and the functional derivative simplifies to an ordinary derivative,

$$\ddot{\phi} + 3H\dot{\phi} + V'(\phi) = 0, \tag{2.4}$$

where primes represent derivatives with respect to the field ϕ. It is often practical to assume that the friction term dominates the acceleration term, i.e., $\ddot{\phi} \ll 3H\dot{\phi}$. This assumption together with (2.2) define the so-called *slow-roll approximation* [29]. Slow roll is conveniently characterized by the conditions $\varepsilon_V < 1, |\eta_V| < 1$, where

$$\varepsilon_V = \frac{m_P^2}{2}\left(\frac{V'(\phi)}{V(\phi)}\right)^2 \tag{2.5}$$

and

$$\eta_V = m_P^2\frac{V''(\phi)}{V(\phi)} \tag{2.6}$$

are the so-called *slow-roll parameters*. The equivalence of these conditions to the previous conditions on (2.4) may be seen by direct substitution. Under slow roll, the scale factor expands as

$$a(t) \propto \exp\left(\int H\,\mathrm{d}t\right) \equiv e^{-N}$$

where we have defined N by the relation $\mathrm{d}N = -H\,\mathrm{d}t$. The parameter N is called the *number of e-folds* and serves as a measure of the amount of expansion that occurs during inflation. In terms of the potential,

$$N = -\int H\,\mathrm{d}t \approx -\int_{\phi_{\text{start}}}^{\phi_{\text{end}}}\frac{V(\phi)}{V'(\phi)}\,\mathrm{d}\phi. \tag{2.7}$$

The integral (2.7) is taken over the interval $[\phi_{\text{end}}, \phi_{\text{start}}]$. A model of inflation should not only provide a potential, but also a mechanism for inflation to end. In many models, ϕ_{end} is taken to be the point at which the slow-roll approximation breaks down. On the other hand, the start of inflation is given by physical considerations. Quantum fluctuations in the inflaton field at the time of inflation were expanded enough to be measurable today as macroscopic observables. (See figure 1.2.) These are currently thought to be responsible for the development of large scale structure such as galaxies, and is considered to be the greatest motivation for inflation. The experimental quantity related to the power spectrum induced by the perturbations may be expressed in terms of the potential, and is given by

$$\Delta_R^2 \approx \frac{1}{24\pi^2}\frac{V}{\varepsilon_V}\bigg|_{\phi_{\text{start}}} \tag{2.8}$$

to first order in slow roll. (See [30] for a derivation of higher order expressions.)

The power spectrum is often approximated by the power law form (with wavenumber k)

$$P_s(k) = A_s(k_0)\left(\frac{k}{k_0}\right)^{n_s(k_0)-1+(1/2)\alpha_s(k_0)\ln(k/k_0)+\ldots},$$

where k_0 is the pivot scale and A_s is an amplitude. If the perturbations are Gaussian, then the power spectrum contains all the information we need. (If the perturbations are non-Gaussian, we would require higher order expressions.) One may show that the scalar *spectral index*, n_s, and the *running* of n_s, α_s are given by

$$n_s \approx 1 - 6\varepsilon_V + 2\eta_V \tag{2.9}$$

and

$$\alpha_s = \frac{dn_s}{d\ln k} \approx 16\varepsilon_V\eta_V - 24\varepsilon_V^2 - 2\xi_V^2 \tag{2.10}$$

to first order in slow roll, respectively. (Note that α_s is suppressed in slow-roll and a detection would be indication of inflation beyond slow roll.) The function

$$\xi_V^2 \approx \frac{V'V''}{V^2} \tag{2.11}$$

is considered a third slow-roll parameter[1]. (In general, the equation for the nth slow-roll parameter is given by [31]

$$\beta_{(n)}^n = m_P^{2n}\frac{(V')^{n-1}(d^{n+1}V/d\phi^{n+1})}{V^n},$$

and the slow-roll conditions are $|\beta_{(n)}^n| \ll 1$.) A flat, scale-invariant (Harrison-Zeldovich) spectrum corresponds to $n_s = 1$, $n_s < 1$ is said to be red-titled, and $n_s > 1$ blue-tilted.

The power spectrum P_s is generated by scalar curvature perturbations. Likewise, the power spectrum P_t is generated by tensor curvature perturbations. The ratio of the amplitudes of the two power spectrums produces the *tensor-to-scalar* ratio, which in slow roll is given by

$$r = \frac{A_t}{A_s} = -8n_t \approx 16\varepsilon_V, \tag{2.12}$$

[1] The function is defined as ξ_V^2 and not ξ_V for historical reasons [29]. The same is true for equation (2.8).

where n_t is the tensor spectral index (defined in an analogous manner to n_s). This is our last, but most important inflationary observable. Section 2.5 is devoted to discussing its implications.

Let us now turn our attention to the inflationary potential itself. Nothing we have said so far has specified or given hints as to the form $V(\phi)$ should take. In fact, inflationary theory itself is completely silent on the matter. The potential can have any form as long as the model agrees with experimental measurements of the inflationary observables. The first models of inflation were reasonably simple, but the form of $V(\phi)$ quickly grew in complexity as physicists began to look to particle physics for natural motivations. Suppose we have a supersymmetric inflationary potential $V(\phi)$ expanded in a power series about the origin,

$$V(\phi) = \underbrace{V_0}_{\text{dominant term}} + \overbrace{\frac{1}{2}m^2\phi^2}^{\text{mass term}} + \lambda_3 m_p \phi^3 + \underbrace{\frac{1}{4}\lambda\phi^4}_{\text{self-interaction term}} + \sum_{d=5}^{\infty} \lambda_d m_P^{4-d}\phi^d + \dots \quad (2.13)$$

At this point we have two options: we may either look towards another theory to restrict the form of the potential or we may try to use observational data to reconstruct $V(\phi)$ numerically [32–46]. As an example of the former, one usually applies internal symmetries which prohibit the cubic term. Additionally, the higher order terms are non-renormalizable and are therefore prohibited if not properly suppressed:

$$V(\phi) = V_0 + \frac{1}{2}m^2\phi^2 + \underbrace{\lambda_3 m_p \phi^3}_{\text{forbidden by symmetry}} + \frac{1}{4}\lambda\phi^4 + \overbrace{\sum_{d=5}^{\infty} \lambda_d m_P^{4-d}\phi^d}^{\text{non-renormalizable}} + \dots$$

It follows from the definition of the slow-roll parameters (2.5) and (2.6) that the slow-roll conditions $\varepsilon_V < 1, |\eta_V| < 1$ may be seen as flatness conditions on the potential. The steeper the potential, the greater in magnitude V', which implies that $\varepsilon_V \propto V'/V$ will increase. It follows that slow-roll requires nearly flat potentials, which may be achieved if the constant term V_0 in (2.13) is dominate. The potential, of course, cannot be perfectly flat or there would be no minimum for the inflaton to roll towards, and, hence, nothing to drive inflation. One method of providing a slight slope to a flat potential is via quantum corrections using the Coleman-Weinberg formula [47] (see appendix B for a discussion). Another method is to postulate that the inflaton has a self-interaction strong enough to give $V(\phi)$ the proper shape.

Of the two, only the slow-roll condition $|\eta_V| < 1$ can be violated, for violating $\varepsilon < 1$ would produce a significant tensor-to-scalar ratio via (2.12). So while not required in theory, the slow-roll approximation is practically mandatory to match experimental data. In particular, it is difficult, but not impossible, to obtain a nearly scale-invariant power spectrum without slow roll. For potentials that do support slow roll, numerically solving the appropriate inflationary equations [48, 49] directly can give higher order results [30] and may be useful when comparing models to measurements of the tensor-to-scalar ratio. Public codes such as `ASPIC` and `FieldInf` [4] are available to compute reheating consistent predictions for inflationary models. This level of accuracy is not taken into account in this work as supersymmetric reheating is currently not well understood.

So far we have discussed inflation in general, but we are really only concerned *observable* inflation. We will not go into the details here, but inflation causes the observable universe to exit and then reenter the horizon. (The interested reader is referred to any book on cosmology.) The result of this is that any information from before reentry is lost to us and cannot be observed. Thus, we are only concerned with inflation that occurred after this point. It is easy to show that the minimum number of e-foldings (2.7) to solve the flatness and horizon problems is around 50-60. (This calculation assumes GUT scale reheating [11].)Hence, we say that there must be a minimum of 50-60 e-foldings, N_0, of observable inflation. A more precise estimate of N_0 for a specific model may be derived by taking into account the statistical mechanics associated with reheating [50].

2.3 Power Law Inflation

An inflationary model starts with a specification of the potential V, or something from which V can be derived. Once the potential is determined, the general procedure is rather simple:

- Use the experimental bounds on equation (2.8) to solve for ϕ_{start}.
- Use the slow-roll conditions to solve for ϕ_{end}.
- Use ϕ_{start} and ϕ_{end} to evaluate the number of observable e-foldings. This should be at least of order 50-60.
- Evaluate (2.9), (2.10), and (2.12) at ϕ_{end} and check against experimental bounds.

Of course one may go further and check other observables and phenomenology such as the level of non-Gaussianity, the cosmic string contribution, reheating constraints, particle physics constraints, etc., but it is not necessary to consider these details at this time. (Note that reheating is (inflationary) model-dependent. Also, a detection of non-Gaussianity would rule out all slow-roll models.)

Before we go any further, it is instructive to provide an example inflationary model. The simplest model and one of the few for which the inflationary observables can be computed analytically is called *power law inflation*. (We do not spend time on physical motivations. For more information on power law inflation, the reader is referred to any book or review concerning inflationary cosmology. Here, we follow the discussion of [51].)

The potential of power law inflation can be expressed in the form

$$V(\phi) = g\phi^n \quad , \quad n > 0,$$

where the coupling g has dimensions of $(\text{mass})^{4-n}$. By requiring that quantum gravity effects are small and imposing the slow-roll conditions above, it is straightforward to derive upper and lower bounds on ϕ:

$$\frac{n\, m_P\sqrt{6}}{12} \ll \phi \ll \left(\frac{\left(m_p\sqrt{8\pi}\right)^4}{g}\right)^{1/n}. \tag{2.14}$$

This forces the coupling g to be small (in Planck units). The number of e-foldings (2.7) is given by

$$N \approx \int \frac{V}{V'}\,\mathrm{d}\phi = \frac{\phi^2}{2n\,m_P^2}, \tag{2.15}$$

where we have absorbed the negative sign into the limits of integration. Denoting by N_{end} the number of e-foldings at the end of observable inflation, equation (2.15) gives

$$\phi_{\text{end}} = \sqrt{2n\,m_P^2 N_{\text{end}}}. \tag{2.16}$$

In these variables, the slow-roll parameters become

$$\varepsilon_V = \frac{n}{4N_{\text{end}}} \quad , \quad \eta_V = \frac{n-1}{2N_{\text{end}}}.$$

From these we obtain the scalar spectral index,

$$n_s \approx 1 - \frac{3n}{2N_{\text{end}}} + \frac{n-1}{N_{\text{end}}}, \tag{2.17}$$

and the tensor-to-scalar ratio,

$$r \approx \frac{4n}{N_{\text{end}}}. \tag{2.18}$$

We now consider the special case of the quadratic and quartic potentials,

$$V(\phi) = \frac{m^2}{2}\phi^2$$

and

$$V(\phi) = \frac{\lambda}{4!}\phi^4,$$

respectively. The coupling $m \ll m_P^2$ has units of mass and $\lambda \ll 1$ is dimensionless. To satisfy the experimental bounds on Δ_R^2 (see chapter 3), equation (2.8) dictates $m \sim 10^{-5}\,m_P$ and $\lambda \sim 10^{-12}\,m_P$. Hence, both couplings are small (in Planck units) as required above. Table 2.1 summarizes the results of equations (2.16)-(2.18) for the quadratic and quartic models with $N_e = 50$ and 60.

We will discuss experimental bounds on n_s and r in the following chapter, but for now it suffices to make a general comment about the results in table 2.1. Converting from the reduced Planck mass to the Planck mass, $M_{PL} = \sqrt{8\pi}m_P$, shows that the

	ϕ_{end}	n_s	r
$n = 2, N_{\text{end}} = 50$	$14.1\ m_P$	0.96	0.16
$n = 2, N_{\text{end}} = 60$	$15.5\ m_P$	0.97	0.13
$n = 4, N_{\text{end}} = 50$	$20.0\ m_P$	0.94	0.32
$n = 4, N_{\text{end}} = 60$	$21.9\ m_P$	0.95	0.27

Table 2.1: The scalar spectral index and the tensor-to-scalar ratio for power law inflation with $n = 2, 4$ and $N_0 = 50, 60$.

field in quadratic and quartic power law inflation takes on trans-Planckian values. As such, these models are called *large-field* models. (They are also called *chaotic inflation* as one may show that the initial conditions ensuring inflation in these models may emerge accidentally [52].) This is problematic for inflation model building since our current laws of physics are widely considered to be incomplete at these energy scales.

2.4 Hybrid Inflation

Models of inflation like those in the previous section are called *single-field* models because one field provides the dominant contribution to the inflationary potential. There is, however, no physical reason that this must be the case. Models of inflation that are not single-field are called *multi-field*, and have inflationary dynamics governed by

$$H^2 = \frac{1}{3m_p^2}\left[\frac{1}{2}\sum_{i=1}^{n}\dot{\phi}_i^2 + V(\phi_{i=1,\ldots,n})\right]$$

and

$$\ddot{\phi}_i + 3H\dot{\phi}_i + \frac{\partial V}{\partial \phi_i} = 0.$$

One popular multi-field model that is particularly successful and well-motivated from a particle physics standpoint is called *hybrid inflation*. (The original hybrid inflation model proposed by Andrei Linde in 1991 and 1994 [53, 54] is no longer viable, but the general concept is still used today.) The standard hybrid model contains two fields which work together to provide successful inflation, but the hybrid concept may be extended to include more fields (see for example [55]). In (standard) hybrid inflation, the inflaton is a slow-rolling field which is coupled to a second field, called the waterfall field, that is fixed during inflation[2]. When the inflaton obtains a critical value the waterfall field undergoes a phase transition (called waterfall) which causes the end of inflation. This critical value is often reached immediately after the η_V slow-roll condition is violated, but this is not detrimental to the model. The waterfall transition is usually assumed to be instantaneous, but this is not mandatory. We will not consider it here, but it is worth noting that non-instantaneous waterfall may nudge inflationary observables outside of current experimental bounds [57]. (Non-Gaussianity is predicted to be small in single-field slow-roll inflation, however, this is not the case for multi-field models or when the slow-roll conditions are violated.)

One significant benefit to hybrid models is that they reduce the number of restrictions on the inflationary potential. To see why, consider the fact that in single field models the potential must both satisfy the slow-roll conditions to drive inflation and then later violate the same conditions to end inflation. Mathematically, there are only a few simple functions which can do this. In hybrid inflation on the other hand, the job of ending inflation is left to the waterfall field, so the only requirement on the potential is that it satisfies slow-roll. Mathematically, this opens a huge range of possibilities for new potentials.

2.5 The Tensor-To-Scalar Ratio

Right now we are lucky enough to live in an era of precision cosmology. A number of CMB experiments, ranging from ground, balloon, to space-based, are expected to release important results within the next few years. One of the most important of these results is a measurement of the tensor-to-scalar ratio (2.12).

The CMB is polarized into two orthogonal components: E-modes and B-modes. E-modes have zero curl and give polarization vectors that are radial around cold spots

[2] Some authors define single-field models to be those with only one field involved in the inflationary dynamics. In this case, hybrid inflation may be thought of as a single-field model since the waterfall field is fixed during inflation. (See for example [56].)

and tangential around hot spots in figure 1.2. B-modes have zero divergence and give polarization vectors that rotate with nonzero vorticity. E-modes can be sourced by scalar and tensor perturbations, while B-modes can be sourced by vector and tensor perturbations. Vector perturbations may be produced by topological defects, whereas tensor B-mode perturbations are identified with a background of primordial gravity waves. Experiments such as Planck can distinguish between gravity waves and topologic defects [58].

The Planck satellite is not sensitive to B-modes and will say the least about r out of all the current and proposed CMB experiments. Limits on r from satellites such as WMAP and Planck are inferred from temperature and temperature-polarization cross-correlation data. Temperature related data can only measure r to an accuracy of 10^{-1} [59]. The best measurements of r will come from B-mode dedicated ground and ballon-based experiments using B-mode autocorrelation data such as BICEP, EBEX, POLARBEAR, SPIDER, and SPUD.

Determining the tensor-to-scalar ratio is of crucial importance in cosmology. An observable r would imply that the field was trans-Planckian at some point during inflation. Most models try to avoid this and, hence, produce small r. All current alternatives to inflation predict an undetectably small value for r. Thus, any detection of r would instantly rule out all of these theories. It is easy for inflation models to satisfy the experimental bounds on n_s, but it is not so easy to satisfy the experimental bounds on r. Therefore, r is an important parameter in distinguishing between models. Any detection of r would instantly rule out a large number of models. The tensor-to-scalar ratio is also related to the energy scale of inflation by $V(\phi_{\mathrm{start}})^{1/4} \approx 3.35 \times 10^{16}$ GeV $r^{1/4}$. This is one of the biggest unknowns in inflationary model building today.

Chapter 3

SUSY HYBRID INFLATION

3.1 Supersymmetric Models of Inflation

In the preceding chapter we discussed models of inflation. We did not discuss motivations for specific models, but everything was based solely only the Standard Model (SM). However, the energy scale of inflation is significantly great enough that it would not be surprising if the SM was no longer valid in this regime. If this were true, inflation would require additional physics beyond the SM such as Grand Unified Theories (GUTs) or supersymmetry (SUSY) (see sections 1.4 and 1.5, respectively). More hints towards the inclusion of physics beyond the SM in inflation come from considering the tensor-to-scalar ratio r (see section 2.5). As previously discussed, if r is great enough to be observable, then the energy scale of inflation is $\sim 10^{16}$ GeV and the inflaton field might be trans-Planckian at some point during inflation [60]. This energy scale is greater than what one would expect coming from SM particle physics phenomenology, but is approximately GUT scale instead. Trans-Planckian fields are also problematic in the sense above where the SM may not be valid. SUSY GUT models of inflation are efficient at ameliorating these issues in a well-motivated manner. All-in-all, by taking particle physics into account one may argue that SUSY models are some of the best inflation models from a phenological perspective. Unfortunately, SUSY inflation models generally predict an unobservable value of the tensor-to-scalar ratio. We will return to this important aspect soon.

3.2 SUSY Hybrid Inflation

The most popular supersymmetric model of inflation is a hybrid model first developed in 1994 [61, 62]. Here, the inflationary sector of the superpotential is an extension of the Higgs mechanism and generates inflation via spontaneous symmetry breaking. It is natural to identify this breaking with already existing phase transitions such as those in GUTs. This puts the energy scale of inflation around $\sim 10^{16}$ GeV, which is compatible with our discussion in the previous chapter. In addition to GUTs, this model may also successfully invoke SUGRA, string theory, and extra dimensions as desired. Fortunately, SUSY hybrid inflation can take place entirely below the Planck scale, which eliminates the need for a complete theory of quantum gravity. Although, as we will see, we will need to invoke SUGRA corrections to match recent experimental data.

The most general non-trivial renormalizable superpotential one can write involving a singlet superfield S and two conjugate supermultiplets Φ (the fundamental representation) and $\bar{\Phi}$ (the anti-fundamental representation) that preserves a gauge group G and $U(1)_R$ R-symmetry is [61, 62]

$$W = \kappa S(\overline{\Phi}\Phi - M^2), \tag{3.1}$$

where M is the energy scale at which G breaks and κ is a dimensionless coupling which we take to be positive without loss of generality since we can absorb the phase of κ into that of S. (Fields not affected by a given symmetry group are said to be a singlet. The inflaton is assumed to be a gauge singlet since gauge coupling are not supposed to be suppressed under SUSY.) We assume a minimal Kähler potential of the form

$$K = |S|^2 + |\overline{\Phi}|^2 + |\Phi|^2. \tag{3.2}$$

The global SUSY F-terms are given by

$$V_F \equiv \sum_i \left| \frac{\partial V_{\text{global}}}{\partial z_i} \right|^2. \tag{3.3}$$

Here, $z_i \in \{s, \phi, \overline{\phi}\}$, where s, ϕ, and $\overline{\phi}$ are the scalar components of the superfields S, Φ, and $\bar{\Phi}$, respectively. We choose to set the D-terms to zero by imposing $|\Phi| = |\overline{\Phi}|$, for convenience.

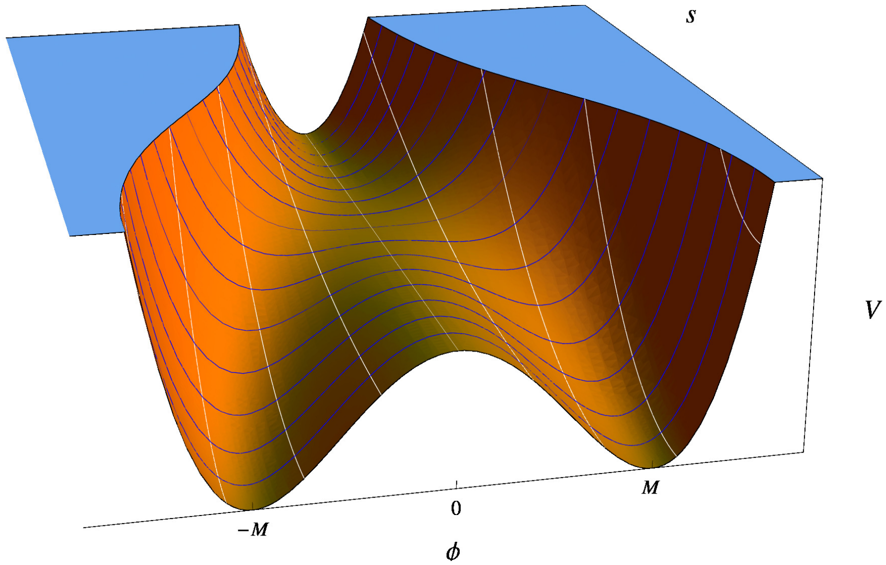

Figure 3.1: The tree-level, global scalar potential V in standard hybrid inflation. The variables s and ϕ are the scalar components of the superfields S and Φ, respectively.

Using equation (3.3), the tree-level global SUSY potential in the D-flat direction is

$$V_F = \kappa^2 \left(M^2 - |\phi|^2\right)^2 + 2\kappa^2 |s|^2 |\phi|^2. \tag{3.4}$$

A plot of this potential in field space is shown in figure 3.1. Inflation proceeds along the local minimum $|\phi| = 0$ (the inflationary track), beginning at large $|s|$ (top of figure 3.1). An instability occurs at the waterfall point $|\tilde{s_c}|^2 = M^2$, which is the value of $|s|$ such that $0 = \left.\frac{\partial^2 V}{\partial |\phi|^2}\right|_{|\phi|=0}$ (the subscript "c" denotes "critical", and the symbol $|\tilde{s_c}|$ will be used later to denote the dimensionful inflaton field at the critical point; we maintain the same notation here for consistency.) At this point the field falls naturally into one of two global minima at $|\phi|^2 = M^2$. This coincides with the breaking of the gauge group G. At large $|s|$, the scalar potential is approximately quadratic in $|\phi|$, whereas at $|s| = 0$ equation (3.4) becomes a Higgs potential.

Along the inflationary track the potential is flat ($V = \kappa^2 M^4$), and thus one cannot drive inflation. One-loop radiative corrections (RC), which should be added for consistency in any case (since SUSY is broken during inflation), can be used to drive inflation. SUSY is restored after inflation, when the field evolves to one of its global minima (where $V = 0$). The radiative corrections [47] involve the function (see appendix **??** for a derivation)

$$F(x) = \frac{1}{4}\left[(x^4+1)\ln\frac{(x^4-1)}{x^4} + 2x^2\ln\frac{x^2+1}{x^2-1} + 2\ln\left(\frac{\kappa^2 m^2 x^2}{Q^2}\right) - 3\right], \tag{3.5}$$

where $x = |s|/|\tilde{s_c}|$ is a convenient reparametrization of the inflaton field, $\mathcal{N}$ is the dimensionality of the representation of the fields Φ and $\overline{\Phi}$, and Q is the renormalization scale. (The tree level approximation is only valid if the couplings of the inflaton to other fields are strongly suppressed.) Altogether, this model is called minimal (F-term) SUSY hybrid inflation and was ruled out in 2006 by the WMAP three-year observations of the scalar spectral index n_s.

The choice to use minimal Kähler in this model is purely for aesthetics as, unlike W, there is no symmetry dictating the form of this potential. It was subsequently shown by Bastero-Gil et al. [63] that relaxing this assumption to its non-minimal form,

$$K = |S|^2 + |\overline{\Phi}|^2 + |\Phi|^2 + \kappa_s\frac{|S|^4}{4m_P^2} + \kappa_{S\Phi}\frac{|S|^2|\Phi|^2}{m_P^2} + \kappa_{S\overline{\Phi}}\frac{|S|^2|\overline{\Phi}|^2}{m_P^2} + \kappa_{SS}\frac{|S|^6}{6m_P^4} + \ldots, \tag{3.6}$$

could bring the model back into agreement with data for $\kappa_S > 0$. Alternatively, [64] was able to achieve the same result while maintaining minimal Kähler by including gravity-mediated soft SUSY breaking terms from minimal supergravity (SUGRA):

$$\Delta V_{\rm soft} = \sum_i M_S^2|z_i| + M_S\left[z_i\frac{\partial W}{\partial z_i} + (A-3)W + \ldots\right]. \tag{3.7}$$

Here, M_S is the mass breaking scale, A is the coefficient of the trilinear term in the effective low-energy Lagrangian, and the dots represent higher order terms. These had previously been shown to be important for particle physics considerations such as the MSSM μ-problem [65]. See [66] for a discussion in relation to SUSY hybrid inflation or [25] for a thorough review.

From (3.1) and (3.7) we retain a linear soft term and a mass-squared soft term, aM_SS and $M_S^2S^2$, respectively, where $a = 2|2-A|\cos[\arg S + \arg(2-A)]$. Note the field S may be complex. The linear term generally dominates the mass term for most of parameter space, and it is common to choose M_S to be equal to the gravitino mass $m_{3/2}$. With this choice of M_S, adding these terms to the minimal SUSY hybrid inflation model agrees with experiment for a negative. Soon after, the same group demonstrated [67] that similar results could be obtained with a positive by allowing M_S to vary as in split-SUSY models [68].

Despite matching experimental data on the scalar spectral index, SUSY inflation generally predicts a tensor-to-scalar ratio far too small to ever be observed. In general, this result is expected due to the Lyth bound, which says that r is observable if and only if the change in the inflaton field is comparable to the reduced Planck mass, i.e. $\Delta S \sim m_P$ [60, 69]. However, this analysis requires certain assumptions about the slow-roll parameters which are not necessarily valid for SUSY hybrid inflation models. Consequently, one may obtain observable gravity waves in this model without trans-Planckian excursions [70]. For example, utilizing non-minimal Kähler and a large soft mass with $\kappa_S, \kappa_{SS}, M_S^2 > 0$ produces $r \sim 0.01$. (See [70] for a discussion of particle physics implications of large r.) Immediately following this work, it was shown that one may achieve the same results by keeping $M_S \sim m_{3/2} \sim 1$ TeV by allowing κ_S negative [71]. This choice of mass scales is more natural from a particle physics perspective in gravity-mediated soft SUSY-breaking models.

With the recent advances in particle physics driven by the Large Hadron Collider, it is important to keep our models firmly grounded in reality. Besides the particle physics considerations discussed above, the superpotential (3.1) is determined by the R-charges assigned in the rest of the superpotential. For example, under flipped $SU(5)$, if [72]

$$\begin{aligned} W = \kappa S\left(\mathbf{10}_H\overline{\mathbf{10}}_H - M^2\right) + \lambda_1\mathbf{10}_H\mathbf{10}_H\mathbf{5}_h + \lambda_2\overline{\mathbf{10}}_H\overline{\mathbf{10}}_H\overline{\mathbf{5}}_h \\ + y_{ij}^{(d)}\mathbf{10}_i\mathbf{10}_j\mathbf{5}_h + y_{ij}^{(u,\nu)}\mathbf{10}_i\overline{\mathbf{5}}_j\overline{\mathbf{5}}_h + y_{ij}^{(e)}\mathbf{1}_i\overline{\mathbf{5}}_j\mathbf{5}_h, \end{aligned}$$

then we may assign the R-charges as

$$(S, \mathbf{10}_H, \overline{\mathbf{10}}_H, \mathbf{5}_h, \overline{\mathbf{5}}_h, \mathbf{10}_i, \overline{\mathbf{5}}_i, \mathbf{1}_i) = (1, 0, 0, 1, 1, 0, 0, 0).$$

This R-symmetry ensures that proton decay occurs only via the six-dimensional operator (the $\mathbf{5}_h\overline{\mathbf{5}}_h$ term is disallowed). The importance of this is that we preclude rapid proton decay. However, one also prohibits terms such as the quartic couplings $\mathbf{10}_i\mathbf{10}_j\overline{\mathbf{10}}_H\overline{\mathbf{10}}_H$, which give rise to right-handed neutrino masses. (Note that the decay of Majorana right-handed neutrinos can explain the observed baryon asymmetry via leptogenesis [73, 74].)

If we reassign R-charges such that $\mathbf{10}_i\mathbf{10}_j\overline{\mathbf{10}}_H\overline{\mathbf{10}}_H$ is allowed, we end up prohibiting the Yukawa term which gives rise to down-type quark masses (${y_{ij}}^{(d)}\mathbf{10}_i\mathbf{10}_j\mathbf{5}_h$). This outcome is not necessarily catastrophic, since the relevant quark masses may be generated radiatively. On the other hand, one may invoke a "double seesaw" mechanism [72] to account for the lack of large right-handed neutrino masses. A simpler solution to this problem is to allow higher-order (Planck scale suppressed) R-symmetry violating terms in the superpotential, while enforcing R-symmetry for renormalizable terms. With this motivation in mind, we wish to explore the effects of these additional terms on the inflationary dynamics. Introducing these terms raises the question of whether such a modified model can support successful inflation in the context of global SUSY alone: we find that this is not the case, leading us to incorporate SUGRA when constructing our model.

3.3 Planck Scale Suppressed R-Symmetry Violation

We now wish to determine the effects of allowing R-symmetry violation beyond the renormalizable level. First, let us list which additional terms one can consider in this type of model. The three lowest-order nonrenormalizable R-violating terms one can write with the aforementioned superfields (respecting gauge symmetry) are

$$\frac{\alpha}{m_P}S^4 \quad , \quad \frac{\beta}{m_P}S^2(\bar{\Phi}\Phi) \quad , \quad \frac{\gamma}{m_P}(\bar{\Phi}\Phi)^2,$$

where α, β, and γ are dimensionless, and are sufficiently small such that each term is a perturbation about the standard case. Along the inflationary track, only the first term will lift the potential. Therefore, in this letter we consider solely the inflationary ramifications of the S^4 term, so that our superpotential is

$$W = \kappa S(\overline{\Phi}\Phi - M^2) + \frac{\alpha}{m_P} S^4. \tag{3.8}$$

Other inflationary tracks may be available via the inclusion the β and γ terms. Inclusion of these terms may lead to a form of shifted inflation; however, we do not discuss this here.

It is important to ask the following question: Can we drive inflation with this S^4 term, without radiative corrections nor any additional terms? Let us compute the global, tree-level scalar potential along the inflationary track. We do this via equation (3.3), which yields the dimensionless potential ($\mathcal{V} \equiv V/{m_P}^4$)

$$\mathcal{V}_F\bigg|_{|\phi|=0} = \kappa^2 m^4 - 8\cos(\theta_\alpha + 3\theta_s)|\alpha|\, x^3 \kappa {s_c}^3 m^2 + 16 x^6 \left|\alpha\right|^2 {s_c}^6, \tag{3.9}$$

where θ_α and θ_s are the phases of α and s, respectively, and where we have defined the following dimensionless parameters:

$$x \equiv \frac{|s|}{|\tilde{s_c}|}, \quad s_c \equiv \frac{|\tilde{s_c}|}{m_P}, \quad m \equiv \frac{M}{m_P}.$$

The symbol $|\tilde{s_c}|$, as before, denotes the inflaton field at the waterfall point and its dimensionless value s_c is given by

$$-\kappa m^2 + {s_c}^2(\kappa + 4|\alpha| s_c) = 0. \tag{3.10}$$

It can be shown that, using just equation (3.9), one cannot obtain a red-tilted spectrum while simultaneously satisfying the slow-roll conditions (to be defined somewhat later). An analytical calculation reveals that, by imposing the condition $n_s < 1$ in the slow-roll approximation, the inflaton field at the start of inflation is necessarily trans-Planckian (see appendix B of [75]). We therefore cannot, in this scenario, achieve a suitable spectral tilt without additional terms. In other words, one cannot have successful inflation using only the global SUSY terms.

In order that our model yield more experimentally favorable results, we include soft and SUGRA corrections to the global plus RC potential. The soft terms are derived in a gravity-mediated SUSY-breaking scenario [25] using (3.7); including the soft mass squared terms, they are

$$a\, m_{3/2}\, \kappa m^2\, s_c x \quad , \quad m_{3/2}{}^2\, s_c{}^2 x^2 \quad , \quad b\, m_{3/2}\, |\alpha|\, s_c{}^4 x^4,$$

where the last term is a direct consequence of our S^4 term in W, and $m_{3/2}$ is the gravitino mass ($\sim$ TeV) divided by m_P. We write the effective coefficients of the soft terms as

$$\begin{aligned} a &= 2\left[2\cos(\theta_s) - |A|\cos(\theta_A + \theta_s)\right], \\ b &= 2\left[|A|\cos(\theta_A + \theta_\alpha + 4\theta_s) + \cos(\theta_\alpha + 4\theta_s)\right], \end{aligned} \tag{3.11}$$

where each θ_i, $i \in \{A, \alpha, s\}$, is the phase of a complex parameter, and A is the trilinear coupling. Note that we cannot take α real without loss of generality, since we have already absorbed the phase of κ into that of s; therefore, we consider the most general case where α, s, and A are complex.

While θ_A and θ_α are components of couplings, θ_s is a dynamical field. For the sake of simplicity, we minimize the potential with respect to θ_s so as to define the inflaton field purely as $|s|$. As a result (see appendix A of [75]), we choose the following values of the phases

$$\theta_s = l\pi \quad , \quad \theta_A = n\pi \quad , \quad \theta_\alpha = p\pi,$$

such that l, n, and p are all odd integers. With these choices, the effective coefficients are

$$a = -2(2 + |A|) \quad , \quad b = 2(|A| - 1),$$

and in conjunction with these phase choices we additionally impose the condition that $|A| < 1$, or equivalently $b < 0$ (see appendix B of [75]). Henceforth, we drop the bars on A and α with the understanding that they represent the moduli of the corresponding complex quantities.

We include SUGRA correction terms up to sixth order in the inflaton field $|s|$, consistent with our inclusion of the $\alpha^2 |s|^6$ global SUSY term; they are:

$$\frac{1}{2}\kappa^2 m^4 s_c{}^4 x^4 \quad , \quad \frac{2}{3} m^4 \kappa^2 s_c{}^6 x^6 \quad , \quad -12\kappa\, m^2\, \alpha\, s_c{}^5 x^5.$$

Hence, with the addition of the soft SUSY-breaking, SUGRA, and 1-loop radiative correction terms to equation (3.9), the full scalar potential, scaled by $1/{m_P}^4$, becomes

$$\begin{aligned}\mathcal{V} &= \kappa^2 m^4 - 8\alpha\,\kappa\,{s_c}^3 m^2 x^3 + 16\,\alpha^2\,{s_c}^6 x^6 + \frac{m^4\kappa^4\mathcal{N}}{8\pi^2}F(x)\\ &+ a\,m_{3/2}\,m^2\,\kappa\,s_c\,x + b\,m_{3/2}\,\alpha\,{s_c}^4 x^4 + {m_{3/2}}^2\,{s_c}^2 x^2\\ &+ \frac{1}{2}m^4\kappa^2{s_c}^4 x^4 + \frac{2}{3}m^4\kappa^2{s_c}^6 x^6 - 12\kappa\,m^2\,\alpha\,{s_c}^5 x^5,\end{aligned} \tag{3.12}$$

where $F(x)$ is given by (3.5).

In solving the essential cosmological equations, we employ the slow-roll approximation throughout, in which inflation occurs while the slow-roll parameters are less than unity. In our notation these are written as

$$\varepsilon = \frac{1}{4{s_c}^2}\left(\frac{\mathcal{V}'}{\mathcal{V}}\right)^2 \quad , \quad \eta = \frac{1}{2{s_c}^2}\frac{\mathcal{V}''}{\mathcal{V}} \quad , \quad \xi^2 = \frac{1}{4{s_c}^2}\frac{\mathcal{V}'''\mathcal{V}'}{\mathcal{V}^2}.$$

Here, the prime ($'$) denotes a derivative with respect to x. Inflation ends either when the slow-roll parameters become unity, or when the inflaton field reaches the waterfall point at $x = 1$. Observable inflation starts at x_0, defined at the pivot scale $k_0 = 0.002$ Mpc^{-1}, and ends at x_e. With this, the number of e-foldings becomes, to leading order,

$$N_0 \approx 2{s_c}^2 \int_{x_e}^{x_0} \frac{\mathcal{V}}{\mathcal{V}'}\,dx, \tag{3.13}$$

while the usual definitions hold for

$$r \approx 16\varepsilon \quad , \quad n_s \approx 1 - 6\varepsilon + 2\eta \quad , \quad \frac{\mathrm{d}n_s}{\mathrm{d}\ln k} \approx 16\varepsilon\,\eta - 24\varepsilon^2 - 2\xi^2. \tag{3.14}$$

The amplitude of the curvature perturbation is given, to leading order, by

$$\Delta^2_{\mathcal{R}} \approx \frac{{s_c}^2}{6\pi^2}\frac{\mathcal{V}^3}{\mathcal{V}'^2}. \tag{3.15}$$

Note that equations (3.14) and (3.15) are evaluated at the pivot scale.

In our numerical calculations we take $m_{3/2} = 1$ TeV$/m_P$, $Q = 10^{15}$ GeV$/m_P$, and since we are implicitly embedding our model in flipped $SU(5)$, we take $\mathcal{N} = 10$ [67]. In addition, we impose the ranges in table 3.1.

Fundamental parameter	Range	Scale type	Derived quantity	Constraining range
κ	$[10^{-6}, 1]$	log	n_s	$[0.9311, 0.9895]$
m	$[10^{-4}, 10^{-1}]$	log		$= 0.9603 \pm 4\sigma$
α	$[10^{-14}, 10^{-8}]$	log	$\Delta^2_{\mathcal{R}}$	$[2.271, 2.583] \times 10^{-9}$
A	$[10^{-10}, 1]$	log		$= 2.427 \times 10^{-9} \pm 2\sigma$
x	$(1, \frac{1}{m}]$	linear	r	< 0.11
s_c	$(0, 1)$	linear	N_0	$[50, 60]$

Table 3.1: These are the ranges specified for the fundamental parameters in equation (3.12), and constraints placed on derived quantities, that we have used in our numerical calculations. Note that x can take on any value between the waterfall point and the Planck scale. The experimental bounds on r, $\Delta^2_{\mathcal{R}}$, and n_s are from the Planck satellite [3]. The numerical constraints on the quantities r and $\Delta^2_{\mathcal{R}}$ are the experimental bounds; however, the numerical constraints on n_s differ slightly from the experimental bounds. This has been done for ease of plotting.

3.4 Results

3.4.1 Overview

Previous studies have shown that small gravity waves are generated using minimal Kähler and a TeV-scale positive soft SUSY-breaking mass squared term (i.e., ${m_{3/2}}^2\, x^2$, with $m_{3/2} \sim 10^{-16}$) [64, 67, 76]. Specifically, when the lowest-order SUGRA correction term and a negative linear soft term ($a = -1$) are added to the global SUSY plus TeV-scale positive soft mass squared plus RC potential, one finds that $r \sim 10^{-12.5}$ around the Planck central value $n_s = 0.9603$ [64]. Alternatively, using non-minimal Kähler in shifted inflation with positive TeV-scale soft mass squared and $a = 1$, 0, or -1 [71, 76–78], or non-minimal Kähler with with same a values, and large, positive soft mass squared terms ($\sim 10^{-5}$) [70], one can generate $r \sim 10^{-2}$ with red spectral tilt. In this paper we find that the solutions follow curves of a similar shape to those presented in [64], as can be seen in figure 3.2. By employing minimal Kähler, positive TeV-scale soft mass squared terms, and a negative linear and a negative α-dependent quartic soft term, we obtain in this paper $r \sim 10^{-8.5}$ around $n_s \simeq 0.9603$ for $\alpha = 10^{-9}$; in [64], one obtains r values four orders of magnitude lower than this, at $n_s \simeq 0.9603$.

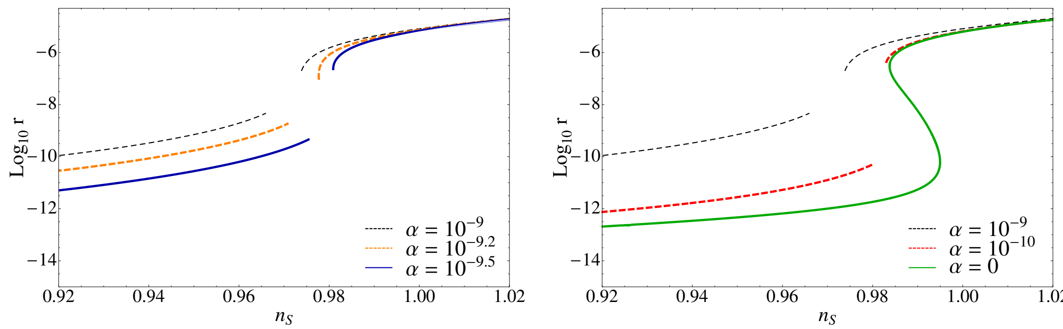

(a) (b)

Figure 3.2: The tensor-to-scalar ratio, r, versus the scalar spectral index, n_s, is depicted. Three curves for large values of α are shown in 3.2(a), and a larger range of α is taken in 3.2(b). Here, the number of e-foldings and A have been fixed at 50 and 10^{-4}, respectively. With $\alpha = 0$, we produce solutions closely matching the $a = -1$ case in [64]. Note that this curve (in 3.2(b)) does not produce false vacua.

As we will describe, this model yields even larger gravity waves ($\sim 10^{-4}$, see figure 3.5(b)) with red spectral tilt, and we expect that with non-minimal Kähler this model can yield solutions similar to [70]. While the full set of results is outside the reach of current experiments such as Planck, a model in which solutions are tending toward larger r solutions is nonetheless preferred.

3.4.2 The Effect of the Parameters on the Model

Our potential is dependent upon the inflaton field x and the parameters A, α, κ, and m. Our new parameter α, which parametrizes the amount of R-symmetry violation beyond the renormalizable level, yields qualitatively and quantitatively distinct results from the standard case.

The negative α-dependent terms in (3.12) create false vacua in some regions of parameter space, i.e. the general behavior of the potential changes from that of figure 3.3(a) to that of 3.3(b). (Note that the inflaton field rolls from right to left in these figures.) We cannot produce a successful inflationary scenario from figure 3.3(b) as the system will become trapped in the false vacuum. Rejecting solutions for which this

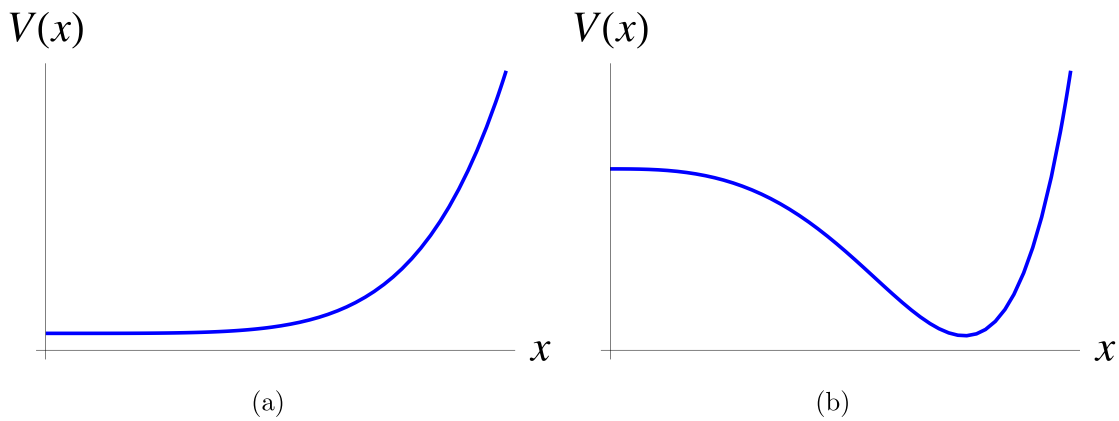

Figure 3.3: The qualitative change in behavior caused by the negative α terms. figure (a) depicts a potential that is well-behaved, i.e., the field will roll toward the global minimum, while figure (b) depicts a potential with a false vacuum. Mathematical solutions which produce false vacua are not acceptable inflationary scenarios.

occurs produces gaps in the parameter space such as those seen in figures 3.2 and 3.7. Note that these vacua did not appear in [64].

Figure 3.2 depicts the effects of α on r. (See figure 3.7 for further results. Note the similarity of these curves to those in [64].) The potential in equation (3.12) differs from that in [64] by two higher-order SUGRA correction terms, an α-dependent quartic soft term, and two global α-dependent terms (a is also different). The effect of α is to raise r, particularly in red-tilted regions. This is primarily a result of the global term proportional to α. The $\alpha = 10^{-9}$ curve is raised by three to six orders of magnitude for $0.92 < n_s < 0.98$, as compared to the $\alpha = 0$ case in [64].

Our model greatly benefits from the fact that we can, as noted, generate larger gravity waves than the standard ($\alpha = 0$) case. However, α cannot be raised arbitrarily, since we require R-symmetry violation to be small. We find no need to impose an upper bound, though, because our parameter study yields a numerical upper bound $\alpha \sim 10^{-7}$. This can be understood mathematically by noting that $|\mathcal{V}'|$ increases faster than $|\mathcal{V}|$ as $\alpha \to 10^{-7}$ (from smaller α). The e-foldings constraint (3.13) becomes impossible to satisfy at large α, because its integrand is suppressed by a large $\mathcal{V}'$, and

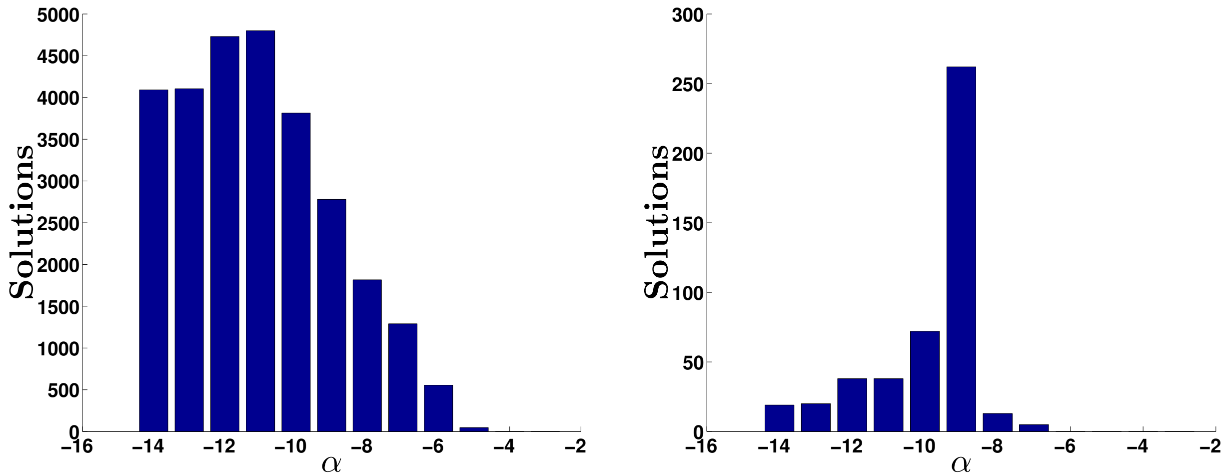

(a) (b)

Figure 3.4: The number of solutions to $\Delta_{\mathcal{R}}^2 = 2.427 \times 10^{-9}$ (a), and both $\Delta_{\mathcal{R}}^2 = 2.427 \times 10^{-9}$ and $N_0 \in [50, 60]$ (b).

the limits of the integral can only be marginally altered.

We find that x_0 can vary over at least two orders of magnitude until $\alpha \sim 10^{-8}$; then, x_0 is compressed to ~ 10. Likewise, the end of inflation is pushed toward waterfall, $x_e = 1$, as $\alpha \to 10^{-7}$. Thus the distance in x over which inflation occurs approaches an approximately constant value. If we take solutions to $\Delta_{\mathcal{R}}^2 = 2.427 \times 10^{-9}$ (figure 3.4(a)) and then impose the constraint that the number of e-foldings be between 50 and 60 (figure 3.4(b)), we observe that, for many orders of magnitude in α, requiring sufficient inflation decreases by at least an order of magnitude the number of solutions relative to those obtained merely from the curvature perturbation constraint. Achieving a sufficient amount of inflation severely limits the number of viable solutions generally, but is most limiting at large α. The curvature perturbation constraint also has a limiting effect as α increases, although notice that without ensuring a sufficient amount of observable inflation, one can obtain "solutions" up to $\alpha = 10^{-5}$ (figure 3.4(a)).

Numerically, we obtained our results using two independent methods: a continuation method and a parameter study. The results of the former are seen in figures 3.2

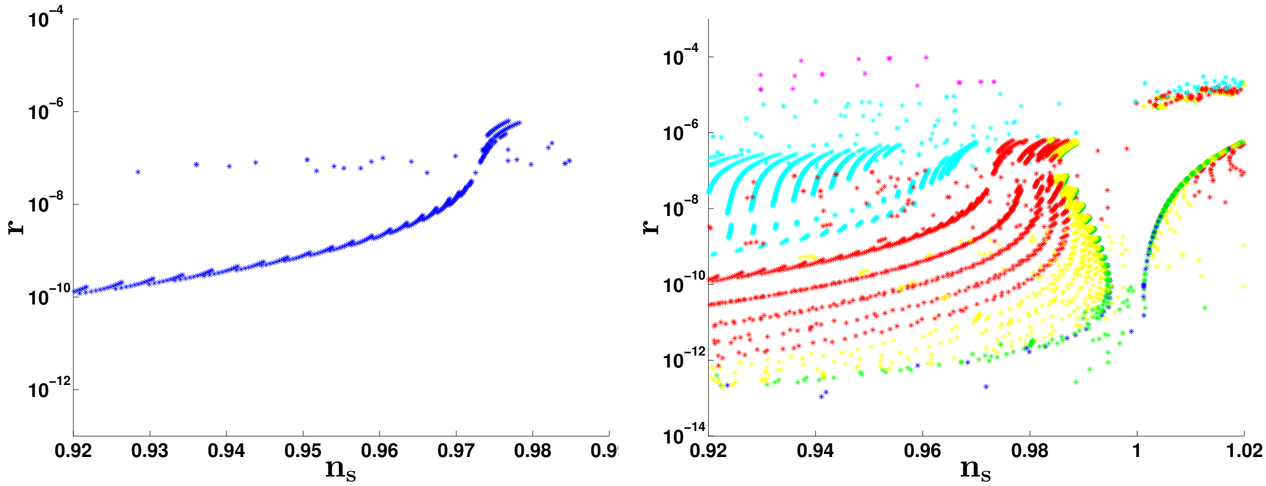

Figure 3.5: (a) The tensor-to-scalar ratio, r, versus the scalar spectral index, n_s, for $\alpha = 10^{-9}$, $A = 10^{-4}$, and $N_0 \in [50, 60]$. One can see the "horizontal solutions", which yield r values somewhat above 10^{-8}. (b) The tensor-to-scalar ratio, r, versus the scalar spectral index, n_s for solutions corresponding to the ranges in table 3.1. Solutions are color-coded as follows: blue - ($10^{-14} < \alpha \leq 10^{-12}$), green - ($10^{-12} < \alpha \leq 10^{-11}$), yellow - ($10^{-11} < \alpha \leq 10^{-10}$), red - ($10^{-10} < \alpha \leq 10^{-9}$), cyan - ($10^{-9} < \alpha \leq 10^{-8}$), magenta - ($10^{-8} < \alpha \leq 10^{-7}$).

and 3.7. The latter results are presented in figures 3.5 and 3.6. Figure 3.5(a) shows the presence of qualitatively new "horizontal solutions" in the $r - n_s$ plane. If we drop all the α-dependent terms in the scalar potential (3.12) except the global term linear in α (which is $-8\alpha\,\kappa\, {s_c}^3 m^2 x^3$), the number of horizontal solutions in this region increases. On the other hand, dropping this term and keeping the others does not produce a viable inflationary scenario. Since the global α term is the most dominant α-dependent term, it is primarily responsible for producing these horizontal solutions.

We find that limits on r naturally arise in our model (see figure 3.6(a)). Solutions producing $r \sim 10^{-4}$ can be produced throughout the range of α that we have taken, although all of these except the solutions near the upper limit of α correspond to a blue-tilted spectrum. Figure 3.5(b) depicts this behavior; note that the only large-r solutions corresponding to red spectral tilt are colored magenta and cyan (meaning

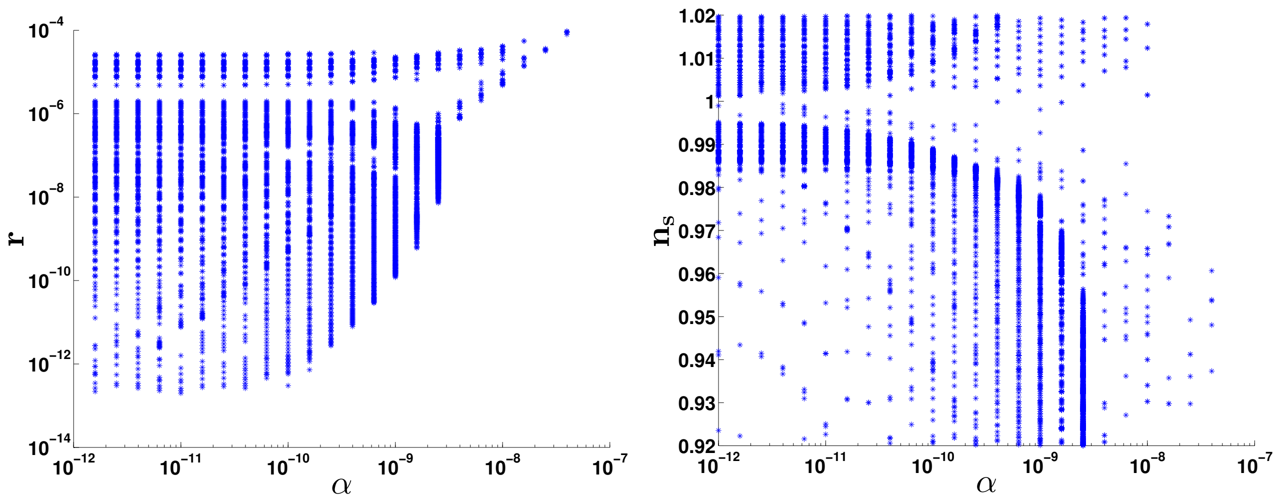

(a) (b)

Figure 3.6: (a) The tensor-to-scalar ratio, r, versus α using the constraints in table 3.1. (b) The scalar spectral index, n_s, versus α using the constraints in table 3.1. Note that in the red-tilted region where $\alpha \to 0$, solutions are sparse.

that $10^{-9} < r \leq 10^{-7}$). Figure 3.6(a) also indicates that the smallest-r solutions that can be produced are increasingly larger as α increases, so that at the upper limit of α only $r \sim 10^{-4}$ can be produced. This effect can be understood by using the following approximation of the energy scale of inflation: ${\mathcal{V}_0}^{1/4} \sim \kappa^{3/2} m^2 / \sqrt{\lambda^2 {x_0}^2 \alpha}$, where $\lambda \equiv [(3456\, \Delta^2_{\mathcal{R}}\big|_{x_0} \pi^2)]^{1/4}$. As mentioned, the integrand in equation (3.13) is suppressed by the fact that $|\mathcal{V}'|$ increases faster than $|\mathcal{V}|$ as α increases. To compensate for this effect the $\kappa^2 m^4$ term in $\mathcal{V}$ increases, raising the numerator in ${\mathcal{V}_0}^{1/4}$. This prohibits small-r solutions in large-α regions (recall that $r \propto {\mathcal{V}_0}^{1/4}$).

The upper limit on r of $\sim 10^{-4}$, approximately constant over many orders of magnitude of α, is a consequence of the Lyth bound [60] $r \lesssim \mathcal{O}(10^{-2}) \times m^2 (x_0 - x_e)^2$. The largest m values obtainable ($m \sim 10^{-1}$) correspond to very small values of $x_0 - x_e$, and therefore limit r below 10^{-4}. Solutions with $m \sim 10^{-2}$ correspond to $x_0 \approx 10$ and $x_e \approx 1$; thus, $m^2 (x_0 - x_e)^2 \sim 10^{-2}$ for the largest r values obtainable in our model.

The parameter A, arising from the gravity-mediated soft-SUSY breaking terms,

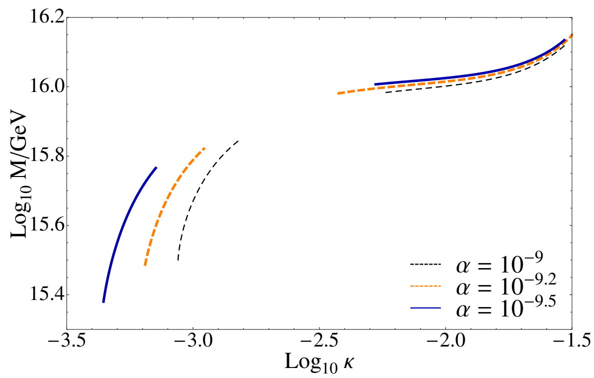

(a)

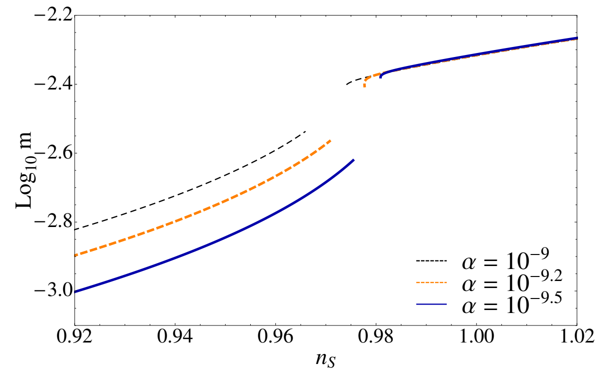

(b)

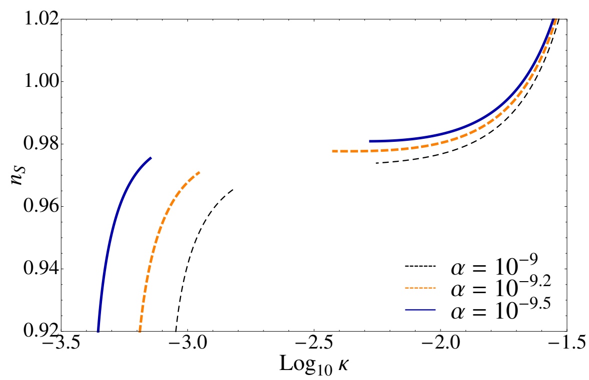

(c)

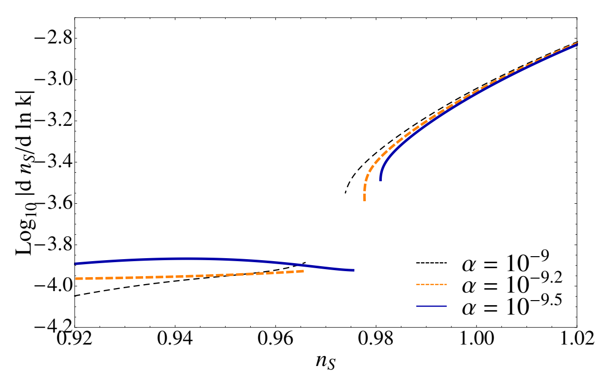

(d)

Figure 3.7: Here we plot our numerical results in which the number of e-foldings and A have been kept fixed at 50 and 10^{-4}, respectively. The absolute value of the running of n_s, $\log_{10}|\frac{\mathrm{d}n_s}{\mathrm{d}\ln k}|$, is plotted in 3.7(d).

does not have any discernible effect on our results in the red-tilted region. This is expected from the fact that the soft terms are suppressed by the gravitino mass ($\sim$ TeV).

The plots in figure 3.7 depict the effects of increasing α. Figures 3.7(a), 3.7(c), and 3.7(d) are in direct reference to [64]. We can see from figure 3.7(c) that large α boosts κ, especially in the red-tilted region. Similarly, figure 3.7(a) shows that, for the same breaking scale M, κ is boosted as α increases. Note that m is also boosted by α (figure 3.7(b)). We have discussed that larger gravity waves are produced via increasing α. This effect is evident from figures 3.7(b) and 3.7(c), which show that

m and κ values are raised as α increases, particularly in red-tilted regions. Figure 3.7(d) depicts the absolute value of the running of n_s, $\log_{10}|\frac{\mathrm{d}n_s}{\mathrm{d}\ln k}|$. In our model, $\frac{\mathrm{d}n_s}{\mathrm{d}\ln k}$ is negative, and $|\frac{\mathrm{d}n_s}{\mathrm{d}\ln k}| \sim \mathcal{O}(10^{-3}) - \mathcal{O}(10^{-4})$.

3.5 BICEP2

The scalar spectral index has been determined by Planck to within 1% and the curvature perturbations to within 4%. These extremely tight experimental bounds have invalidated a large number of inflationary models. Next, physicists hope to determine the running of n_s and the tensor-to-scalar ratio. As far as we can tell, the running is approximately zero and may be slightly negative. On the other hand, recent claims by the BICEP2 experiment suggest that the tensor-to-scalar ratio may be as large as ~ 0.2. This announcement has been received with caution by the physics community, and is awaiting independent verification by Planck in the next year or so. Should, however, it be found that r is indeed in-fact observable, this could be a serious problems for supersymmetric hybrid inflation and other SUSY inflation models, which generally predict small r. Also, it is noteworthy to mention that once r is measured, it has been suggested that it will no longer be adequate to specify an inflationary scenario without a description of reheating [79]. This subject is currently not well understood for SUSY inflation models.

Recent work has focused on raising the tensor-to-scalar ratio for these models. It has been shown, most notably in [80, 81], that it is possible with a clever choice of potential. One difficulty that arises here is that certain parameters are either directly or indirectly constrained by experimental observations of non-inflationary data. For example, it would be convenient to arbitrarily choose κ and M as large as needed, but κ is indirectly constrained through M, which is directly constrained by current bounds on cosmic strings [10]. Employing non-minimal Kähler and postulating the inclusion of more correctional terms coming from particle physics or currently unknown Planck-scale physics often introduces unconstrained parameters into the model. This is harmful to the predictive power of the model and can often lead to problems with fine-tuning and naturalness. Nevertheless, SUSY hybrid inflation has been shown to have the ability to match the BICEP2 results if necessary. This measurement is in tension with Planck data [82], so inflation model builders will revisit this issue more sincerely if it is confirmed.

Bibliography

[1] A.H. Guth, Physical Review D 23, 2 (1981).

[2] G.F. Hinshaw et al., The Astrophysical Journal (2012).

[3] P.A.R. Ade et al., arXiv:1303.5082 (2013).

[4] J. Martin, C. Ringeval, and V. Vennin, Physics of the Dark Universe (2014).

[5] A.A. Penzias and R.W. Wilson, The Astrophysical Journal 142 (1965).

[6] G.F. Smoot et al., The Astrophysical Journal 396 (1992).

[7] C.L. Bennett et al., The Astrophysical Journal 396 (1992).

[8] E.L. Wright et al., The Astrophysical Journal 396 (1992).

[9] P.A.R. Ade et al., arXiv:1303.5086 (2013).

[10] P.A.R. Ade et al., arXiv:1303.5085 (2013).

[11] V.F. Mukhanov, *Physical Foundations Of Cosmology*, Cambridge University Press, 2005.

[12] T.W. Kibble, Journal of Physics A: Mathematical and General 9, 8 (1976).

[13] H. Georgi and S.L. Glashow, Physical Review Letters 32, 8 (1974).

[14] H. Georgi, "The State Of The Art-Gauge Theories", in: *Particles and Fields*, vol. 23, 1974, pp. 575–582.

[15] J. Baez and J. Huerta, Bulletin of the American Mathematical Society 47, 3 (2010).

[16] S.M Barr, Physics Letters B 112, 3 (1982).

[17] R. Jeannerot, Physical Review D 53, 10 (1996).

[18] J.P. Derendinger, J.E. Kim, and D.V. Nanopoulos, Physics Letters B 139, 3 (1984).

[19] L. Susskind, Phys. Rev. D 20 (1979).

[20] G. Aad et al., Physics Letters B 716, 1 (2012).

[21] E.D. Stewart, Phys. Rev. D 56 (1997).

[22] J. Martin et al., Journal of Cosmology and Astroparticle Physics 2014, 03 (2014).

[23] G.F. Giudice and A. Masiero, Physics Letters B 206, 3 (1988).

[24] D.H. Lyth and A. Riotto, Physics Reports 314, 1 (1999).

[25] H.P. Nilles, Physics Reports 110, 1 (1984).

[26] S.P. Martin, *A Supersymmetry Primer*, vol. 1, World Scientific, Singapore, 2010.

[27] A.D. Linde, Physics Letters B 108, 6 (1982).

[28] A. Albrecht and P.J. Steinhardt, Physical Review Letters 48, 17 (1982).

[29] A.R. Liddle, P. Parsons, and J.D. Barrow, Physical Review D 50, 12 (1994).

[30] E.D. Stewart and D.H. Lyth, Physics Letters B 302, 2 (1993).

[31] D.H. Lyth, "Particle Physics Models Of Inflation", in: *Inflationary Cosmology*, Springer, 2007, pp. 81–118.

[32] H.M. Hodges and G.R. Blumenthal, Physical Review D 42, 10 (1990).

[33] E.J. Copeland et al., Physical Review D 48, 6 (1993).

[34] E.J. Copeland et al., Physical Review D 49, 4 (1994).

[35] A.R. Liddle and M.S. Turner, Physical Review D 50, 2 (1994).

[36] J.E. Lidsey et al., Reviews of Modern Physics 69, 2 (1997).

[37] R. Easther and W.H. Kinney, Physical Review D 67, 4 (2003).

[38] M.S. Turner and M. White, Physical Review D 53, 12 (1996).

[39] A.R. Liddle and M.S. Turner, Physical Review D 54, 4 (1996).

[40] J.M. Cline and L. Hoi, Journal of Cosmology and Astroparticle Physics 2006, 06 (2006).

[41] H.V. Peiris and R. Easther, Journal of Cosmology and Astroparticle Physics 2006, 07 (2006).

[42] H.V. Peiris and R. Easther, Journal of Cosmology and Astroparticle Physics 2006, 10 (2006).

[43] A. García, A. Macías, and E.W. Mielke, Physics Letters A 229, 1 (1997).

[44] I.J. Grivell and A.R. Liddle, Physical Review D 61, 8 (2000).

[45] E.W. Mielke, O. Obregón, and A. Macías, Physics Letters B 391, 3 (1997).

[46] E.W. Mielke and F.E. Schunck, Phys. Rev. D 52 (1995).

[47] S. Coleman and E. Weinberg, Physical Review D 7, 6 (1973).

[48] V.F. Mukhanov, JETP Letters 41 (1985).

[49] M. Sasaki, Progress of Theoretical Physics 76, 5 (1986).

[50] A.R. Liddle and D.H. Lyth, *Cosmological Inflation and Large-Scale Structure*, Cambridge University Press, 2000.

[51] D.S. Gorbunov and V.A. Rubakov, *Introduction To The Theory Of The Early Universe: Cosmological Perturbations And Inflationary Theory*, World Scientific, 2011.

[52] A.D. Linde, Physics Letters B 129, 3 (1983).

[53] A.D. Linde, Physics Letters B 259, 1 (1991).

[54] A.D. Linde, Physical Review D 49, 2 (1994).

[55] S. Antusch, D. Nolde, and M.U. Rehman, Journal of Cosmology and Astroparticle Physics 2012, 08 (2012).

[56] D. Baumann et al., arXiv:0811.3919 (2008).

[57] S. Clesse, B. Garbrecht, and Y. Zhu, Physical Review D 89, 6 (2014).

[58] J. Urrestilla et al., Journal of Cosmology and Astroparticle Physics 2011, 12 (2011).

[59] L. Verde, H.V. Peiris, and R. Jimenez, Journal of Cosmology and Astroparticle Physics 2006, 01 (2006).

[60] D.H. Lyth, Physical Review Letters 78, 10 (1997).

[61] G. Dvali, Q. Shafi, and R. Schaefer, Physical Review Letters 73, 14 (1994).

[62] E.J. Copeland et al., Physical Review D 49, 12 (1994).

[63] M. Bastero-Gil, S.F. King, and Q. Shafi, Physics Letters B 651, 5 (2007).

[64] M.U. Rehman, Q. Shafi, and J.R. Wickman, Physics Letters B 683, 2-3 (2010).

[65] G. Dvali, G. Lazarides, and Q. Shafi, Physics Letters B 424, 3 (1998).

[66] J. Wickman, Unpublished (Ph.D Dissertation) (2012).

[67] M.U. Rehman, Q. Shafi, and J.R. Wickman, Physics Letters B 688, 1 (2010).

[68] G.F. Giudice and A. Romanino, Nuclear Physics B 699, 1 (2004).

[69] D.H. Lyth and A.R. Liddle, *The Primordial Density Perturbation: Cosmology, Inflation And The Origin Of Structure*, Cambridge University Press, 2009.

[70] Q. Shafi and J.R. Wickman, Physics Letters B 696, 5 (2011).

[71] M.U. Rehman, Q. Shafi, and J.R. Wickman, Physical Review D 83, 6 (2011).

[72] B. Kyae and Q. Shafi, Physics Letters B 635, 5 (2006).

[73] M. Fukugita and T. Yanagida, Physics Letters B 174, 1 (1986).

[74] G. Lazarides and Q. Shafi, Physics Letters B 258, 3 (1991).

[75] M. Civiletti et al., Physical Review D 88, 10 (2013).

[76] M. Civiletti et al., Physical Review D 84, 10 (2011).

[77] M.U. Rehman and Q Shafi, Physical Review D 86, 2 (2012).

[78] M.U. Rehman, V.N. Şenoğuz, and Q. Shafi, Physical Review D 75, 4 (2007).

[79] J. Martin, C. Ringeval, and V. Vennin, arXiv:1407.4034 (2014).

[80] M. Civiletti, C. Pallis, and Q. Shafi, Physics Letters B 733 (2014).

[81] C. Pallis and Q. Shafi, arXiv:1405.7645 (2014).

[82] J. Martin et al., arXiv:1405.7272 (2014).

Appendix A

THE COLEMAN-WEINBERG FORMULA

Here, we review the basic idea behind the Coleman-Weinberg formula by reproducing the first example of [47].

Consider a massless, quartically, self-interacting (real) meson field ϕ:

$$\mathcal{L} = \frac{1}{2}\left(\partial_\mu \phi\right)^2 - \frac{\lambda}{4!}\phi^4.$$

We wish to find the potential $V(\phi_0)$ for some position independent field $\phi_0(x) = \phi_0$. (One might naïvely assume that this would be $V(\phi_0) = \frac{\lambda}{4!}\phi_0^4$, but this would be treating ϕ as a coordinate, ignoring its self-interaction.) To do this, we treat ϕ_0 as a perturbation of the field ϕ. This implies we find $V(\phi + \phi_0)$ and then integrate out ϕ. From the Lagrangian,

$$\begin{aligned} V(\phi + \phi_0) &= \frac{\lambda}{4!}\left(\phi + \phi_0\right)^4 \\ &= \frac{\lambda}{4!}\phi_0^4 + \frac{\lambda}{6}\phi_0^3\phi + \frac{\lambda}{4}\phi_0^2\phi^2 + \frac{\lambda}{6}\phi_0\phi^3 + \frac{\lambda}{4!}\phi^4. \end{aligned}$$

To zeroth order we have $V(\phi_0) = \frac{\lambda}{4!}\phi_0^4$. The first-order term $\frac{\lambda}{6}\phi\phi_0^3$ implies the Feymann diagram figure A.1 with vertex rule $\frac{\lambda}{3}\phi_0^3$. Computing the diagram gives no contribution to the potential.

Figure A.1: Tree-level diagram.

At second order, $\frac{1}{2}\left(\frac{\lambda}{2}\phi_0^2\right)\phi^2$, we obtain the following 1-loop diagrams with vertex rule $\frac{\lambda}{2}\phi_0^2$ (figure A.2):

Figure A.2: 1-loop diagrams.

$$\begin{aligned}
&= i\int \frac{\mathrm{d}^4k}{(2\pi)^4}\left[\frac{1}{2}\left(\frac{\lambda}{2}\phi_0^2\frac{1}{k^2+i\varepsilon}\right)+\frac{1}{2\cdot 2}\left(\frac{\lambda}{2}\phi_0^2\frac{1}{k^2+i\varepsilon}\right)^2+\frac{1}{2\cdot 3}\left(\frac{\lambda}{2}\phi_0^2\frac{1}{k^2+i\varepsilon}\right)^2+\dots\right] \\
&= i\int \frac{\mathrm{d}^4k}{(2\pi)^4}\sum_{n=1}^{\infty}\frac{1}{2n}\left(\frac{\lambda}{2}\phi_0^2\frac{1}{k^2+i\varepsilon}\right)^n.
\end{aligned}$$

Rotating into Euclidean space, we recognize this as the series expansion for the natural logarithm,

$$=\frac{1}{2}\int\frac{\mathrm{d}^4k}{(2\pi)^4}\ln\left(1+\frac{\lambda\phi_0}{2k^2}\right).$$

This is divergent so we introduce the cutoff Λ,

$$\frac{1}{2}\int_0^\Lambda\frac{\mathrm{d}^2k}{(2\pi)^4}k^2\ln\left(1+\frac{\lambda\phi_0}{2k^2}\right).$$

This is easily computed by letting $x = k^2$, expanding the logarithm into two terms, and integrating by parts. Therefore, to 1-loop we have

$$V(\phi_0)=\frac{\lambda}{4!}\phi_0^4+\frac{\lambda\Lambda^2}{64\pi^2}\phi_0^2+\frac{\lambda^2}{256\pi^2}\phi_0^4\left[\ln\left(\frac{\lambda\phi_0^2}{2\Lambda^2}\right)-\frac{1}{2}\right]. \tag{A.1}$$

The terms proportional to ϕ^3 and ϕ^4 represent higher order corrections and are ignored.

At this point we need to specify our cutoff scale Λ. Equation (A.1) is divergent as $\Lambda\to\infty$, so we renormalize:

$$V(\phi_0)=\frac{\lambda}{4!}\phi_0^4+\frac{1}{2}B\phi_0^2+\frac{1}{4!}C\phi_0^4+\frac{\lambda\Lambda^2}{64\pi^2}\phi_0^2+\frac{\lambda^2}{256\pi^2}\phi_0^4\left[\ln\left(\frac{\lambda\phi_0^2}{2\Lambda^2}\right)-\frac{1}{2}\right].$$

(Note that a mass renormalizable term is present, even though we are studying a massless field theory. This is because "the theory processes no symmetry that would generate vanishing bare mass in the limit of vanishing renormalized mass." [47]) We need to determine the unknowns B and C. Since B is a mass term, is natural to require that $\left.\frac{\partial^2 V}{\partial \phi_0^2}\right|_{\phi_0=0} = 0$. This gives $B = -\frac{\lambda\Lambda}{32\pi^2}$. On the other hand, $\left.\frac{\partial^4 V}{\partial \phi_0^4}\right|_{\phi_0=0}$ does not exist. Thus, to determine C we evaluate $\frac{\partial^2 V}{\partial \phi_0^2}$ at another point Q. This point is arbitrary, but it will be convenient to take the point to be a natural scale for the problem. For convenience, we choose the requirement that $\left.\frac{\partial^2 V}{\partial \phi_0^2}\right|_{\phi_0=0} = \lambda$. This gives $C = -\frac{3\lambda^2}{32\pi^2}\left[\ln\left(\frac{\lambda Q^2}{2\Lambda^2}\right) + \frac{11}{3}\right]$. From (A.1) we have

$$V(\phi_0) = \frac{\lambda}{4!}\phi_0^4 + \frac{\lambda^2}{256\pi^2}\phi_0^4\left[\ln\left(\frac{\phi_0^2}{Q^2}\right) - \frac{25}{6}\right].$$

Notice that Λ has dropped out as required, but the price we pay for this is the Q has dimensions of mass - the original dimensionless theory has obtained a characteristic scale!

In their paper, Coleman and Weinberg point out that, in this example, the minima lie outside the validity of the 1-loop approximation, but this is certainly not the case in general. This example may be generalized to include more complicated field theories. Keeping everything as general as possible produces the Coleman-Weinberg formulas, which are simply the results of computing the 1-loop integrals as above.

Appendix B

DERIVATION OF RADIATIVE CORRECTIONS IN SUPERSYMMETRIC HYBRID INFLATION

Here, we present a derivation of equation (3.5). We begin with the Coleman-Weinberg formula

$$\Delta V_{\text{1-loop}} = \frac{1}{64\pi^2} \sum_{i,j} (-1)^{2j}(1+2j)\mathcal{M}_i^4 \left[\ln\left(\frac{\mathcal{M}_i}{Q}\right)^2 - \frac{3}{2}\right],$$

where Q is some renormalization mass, $\mathcal{M}_i$ is the i-th eigenvalue of the mass matrix, and the sum runs over all helicity states of the fields. Each superfield of (**??**) contains a complex scalar (2 states) and a spin-1/2 Dirac fermion (4 states). Thus, in our case, the sum breaks up into two parts, one for the scalars and one for the fermions: $\Delta V_{\text{1-loop}} = \Delta V_{\text{S}} + \Delta V_{\text{F}}$.

For the scalars we find

$$\Delta V_{\text{S}} = \frac{1}{64\pi^2} \sum_i \mathcal{M}_i^4 \left[\ln\left(\frac{\mathcal{M}_i}{Q}\right)^2 - \frac{3}{2}\right] = \frac{1}{128\pi^2} \sum_i \mathcal{M}_i^4 \left[\ln\left(\frac{\mathcal{M}_i}{Q}\right)^4 - 3\right].$$

The scalar mass matrix is given by

$$\mathcal{M}_{ij}^2 = \frac{\partial^2 V}{\partial z_i \partial z_j},$$

where $z_i \in \left\{s, \overline{s}, \phi, \overline{\phi}\right\}$. Taking the D-flat direction and assuming our scaling, the eigenvalues are

$$\mathcal{M}_i^2 \in \left\{\kappa^2 m^2 \left(x^2-1\right), \kappa^2 m^2 \left(x^2+1\right), -\kappa^2 m^2 \left(x^2-1\right), -\kappa^2 m^2 \left(x^2+1\right)\right\}.$$

Plugging in we get

$$
\begin{aligned}
\Delta V_{\mathrm{S}} =&\frac{1}{128\pi^2}\left\{2\kappa^4 m^4\left(x^2-1\right)^2\left[\ln\left(\frac{\kappa^2 m^2\left(x^2-1\right)}{Q^2}\right)^2-3\right]\right.\\
&\left.+\,2\kappa^4 m^4\left(x^2+1\right)^2\left[\ln\left(\frac{\kappa^2 m^2\left(x^2+1\right)}{Q^2}\right)^2-3\right]\right\}\\
=&\frac{\kappa^4 m^4}{64\pi^2}\left\{\left(x^4-2x^2\right)\left[\ln\left(\frac{\kappa^2 m^2\left(x^2-1\right)}{Q^2}\right)^2-3\right]+\ln\left[\frac{\kappa^4 m^4}{Q^4}x^4+\frac{\kappa^4 m^4}{Q^4}\left(1-2x^2\right)\right]\right.\\
&\left.+\left(x^4+2x^2\right)\left[\ln\left(\frac{\kappa^2 m^2\left(x^2+1\right)}{Q^2}\right)^2-3\right]+\ln\left[\frac{\kappa^4 m^4}{Q^4}x^4+\frac{\kappa^4 m^4}{Q^4}\left(1+2x^2\right)\right]-3\right\}.
\end{aligned}
$$

Let us simplify this expression. To do this, note that

$$
\begin{aligned}
&\left(x^4-2x^2\right)\left[\ln\left(\frac{\kappa^2 m^2\left(x^2-1\right)}{Q^2}\right)^2-3\right]+\left(x^4+2x^2\right)\left[\ln\left(\frac{\kappa^2 m^2\left(x^2+1\right)}{Q^2}\right)^2-3\right]\\
&\qquad=2x^4\ln\left[\frac{\kappa^2 m^2}{Q^2}\left(x^4-1\right)\right]+4x^2\ln\left(\frac{x^2+1}{x^2-1}\right)-6x^4,
\end{aligned}
$$

and

$$
\begin{aligned}
\ln\left[\frac{\kappa^4 m^4}{Q^4}x^4+\frac{\kappa^4 m^4}{Q^4}\left(1-2x^2\right)\right]&=\ln\left[\frac{\kappa^4 m^4}{Q^4}x^4\left(1+\frac{1-2x^2}{x^4}\right)\right]\\
&=\ln\left(\frac{\kappa^4 m^4}{Q^4}x^4\right)+\ln\left(1+\frac{1-2x^2}{x^4}\right)\\
\ln\left[\frac{\kappa^4 m^4}{Q^4}x^4+\frac{\kappa^4 m^4}{Q^4}\left(1+2x^2\right)\right]&=\ln\left(\frac{\kappa^4 m^4}{Q^4}x^4\right)+\ln\left(1+\frac{1+2x^2}{x^4}\right).
\end{aligned}
$$

This produces

$$
\begin{aligned}
\Delta V_{\mathrm{S}} =&\frac{\kappa^4 m^4}{64\pi^2}\left[2x^4\ln\left(x^4-1\right)+4x^2\ln\left(\frac{x^2+1}{x^2-1}\right)-6-6x^4\right.\\
&\left.+\,4\ln\left(\frac{\kappa^2 m^2}{Q^2}x^2\right)+\ln\left(1+\frac{1+2x^2}{x^4}\right)+\ln\left(1+\frac{1-2x^2}{x^4}\right)\right].
\end{aligned}
$$

The fermion mass matrix is defined as

$$
\mathcal{M}_{ij}=\frac{\partial^2 W}{\partial Z_i \partial Z_j}\Big|_{Z_i\to z_i},
$$

giving

$$
\mathcal{M}_i\in\{\pm\kappa m x\}.
$$

As before, we find

$$\Delta V_{\mathrm{F}} = \frac{1}{64\pi^2}(-1)(2)\left(\kappa^2 m^2 x^2\right)^2(2)\left[\ln\left(\frac{\kappa^2 m^2 x^2}{Q^2}\right) - \frac{3}{2}\right] = \frac{\kappa^4 m^4}{32\pi^2}\left[3x^4 - x^4\ln\left(\frac{\kappa^4 m^4 x^4}{Q^4}\right)\right]$$

Therefore,

$$\begin{aligned}\Delta V_{\text{1-loop}} =& \Delta V_{\mathrm{S}} + \Delta V_{\mathrm{F}} \\ =& \frac{\kappa^4 m^4}{32\pi^2}\left[2x^2\ln\left(\frac{x^2+1}{x^2-1}\right) - x^4\ln x^4 + x^4\ln\left(x^4-1\right) + 2\ln\left(\frac{\kappa^2 m^2 x^2}{Q^2}\right)\right. \\ &\left. + \frac{1}{2}\ln\left[\left(1+\frac{1+2x^2}{x^4}\right)\left(1+\frac{1-2x^2}{x^4}\right)\right] - 3\right].\end{aligned}$$

Simplifying and noting that

$$\left(1+\frac{1+2x^2}{x^4}\right)\left(1+\frac{1-2x^2}{x^4}\right) = \frac{\left(x^4-1\right)^2}{x^8}$$

produces the desired result.

The factor of $\mathcal{N}$ in equation (3.5) takes into account that gauge symmetry is intact during inflation, i.e., there are $\mathcal{N}$ copies of each field, where $\mathcal{N}$ is the dimensionality of the gauge supermultiplets $\mathbf{\Phi}, \overline{\mathbf{\Phi}}$.

Appendix C

USEFUL RESULTS FROM HOMOTOPY THEORY

The following is a collection of common results useful in the study of topological defects. The interested reader is referred to any text on homotopy theory.

Theorems And Definitions:

$\pi_0(X)$ is the set of connected components of X

$\pi_1(X)$ is the set of homotopically inequivalent loops in X

$\pi_2(X)$ is the set of homotopically inequivalent closed surfaces in X

Z_n is a set of n points. It does not contain loops or surfaces. Therefore, the only non-trivial homotopy group is $\pi_0(Z_n) = Z_n$.

The (reductive) rank of a compact Lie Group G is the dimension of a maximal torus in G.

Properties:

$S^N = O(N+1)/O(N) = SO(N+1)/SO(N)$

$S^{2k+1} = U(k+1)/U(k)$ for k odd, $k \geq 3$

$\text{rank}(SO(2n)) = \text{rank}(SO(2n+1)) = n$

$\text{rank}(U(n)) = n$

$\text{rank}(SU(n)) = n - 1$

If M is a simply-connected topological space, then $\pi_0(M) = \pi_1(M) = 0$ and $\pi_1(M/H) = \pi_0(H)$. If $\pi_k(H) = \pi_{k-1}(H) = 0$, then $\pi_k(M/H) = \pi_k(M)$.

$\pi_q(X_1 + X_2) = \pi_q(X_1) \times \pi_q(X_2)$

$$\pi_q(S^N) = \begin{cases} 0 & \text{if } q < N \\ Z & \text{if } q = N \end{cases}, \qquad 0 = \{e\} \text{ is the trivial group}$$

The product of maximal tori is a maximal tori of the product. This implies

$\text{rank}(H_1 \times H_2 \times \ldots \times H_n) = \text{rank}(H_1) + \text{rank}(H_2) + \ldots + \text{rank}(H_n)$

	S^1	S^2	S^3	S^4	$SO(2)$	$SO(3)$	$SO(4)$	$SO(n \geq 5)$
π_0	0	0	0	0	0	0	0	0
π_1	Z	0	0	0	Z	Z_2	Z_2	Z_2
π_2	0	Z	0	0	0	0	0	0
π_3	0	Z	Z	0	0	Z	$Z \times Z$	Z

	$U(1)$	$SU(2)$	$SU(3)$	$SU(4)$	$SU(5)$	E_6	E_8
π_0	0	0	0	0	0		
π_1	Z	0	0	0	0	0	0
π_2	0	0	0	0	0	0	0
π_3	0	Z	Z	Z	Z	Z	Z

Table C.1: Homotopy groups of Lie groups commonly utilized in high energy theory.

Results:

The determination of non-trivial homotopy groups may be done using exact sequences. (See table C.1 above.)